pore), anti-Nanog (ab21603; Abcam), and anti-Oct3/4 (sc-5279; Santa Cruz Biotechnology Inc.).

Flow cytometry. FITC-, PE-, PE-Cy7-, APC-, APC-Cy7-, or Pacific Blue-conjugated mAbs were purchased from BD Biosciences or eBioscience and are listed in Supplemental Table 2. Flow cytometry was performed using FACSCalibur and FACSAria (BD) with FlowJo software (Tree Star). The purity of sorted cells was usually greater than 99%.

Bisulfite DNA sequencing analysis. Genomic DNA was purified from ESCs, iPSCs, and MEFs by using the Allprep DNA/RNA Mini Kit (QIAGEN), and 2 μg of DNA was utilized for bisulfite conversion by using the EpiTect Bisulfite Kit (QIAGEN), according to the supplier's protocol. Bisulfite-treated DNA was amplified by PCR and cloned into the pCR 2.1-TOPO vectors (Invitrogen); positive clones were examined by DNA sequencing using the BigDye Terminator v3.1 Cycle Sequencing Kit (ABI), following the vendor's instructions. Sequences extracted from individual clones were then analyzed to reveal the status of CpG methylation for the *Oct3/4* and *Nanog* loci (15).

Correlation analysis of microarrays. Gene expression detected by using microarrays was normalized by the quantile normalization method (29). Pearson's correlation values of logarithms of all signal intensities from 45,101 probes were calculated, and we performed hierarchal clustering of correlation matrices to indicate the degree of similarity between cell types. Scatter diagrams (Supplemental Figure 2) were drawn to display how similarly or differently genes were expressed in 2 samples. These diagrams contain only probes whose signals were present.

Generation of NKT cells from iPSCs. OP9/control and OP9/Dll-1 were used as a monolayer with OP9 medium (α-MEM supplemented with 20% FCS [HyClone], 10 U/ml penicillin, 100 μg/ml streptomycin, and 2.2 g/l of sodium bicarbonate). In brief, iPSCs (iPSC-7a, iPSC-7g, or iPSC-14k; 5×10^4) were cultured with OP9/Dll-1 as an adherent cell layer in OP9 medium. On day 6 of culture, most iPSC colonies were disrupted by treatment with 0.25% trypsin (Invitrogen). The nonadherent cells were then cultured for another 4 days on a fresh OP9/Dll-1 in OP9 medium with the addition of Flt3L (10 ng/ml; Peprotech). On day 10 of culture and every 4 days thereafter, nonadherent iPSC-derived hematopoietic cells were cultured on a fresh OP9/Dll-1 in OP9 medium with Flt3L (10 ng/ml; Peprotech) and IL-7 (1 ng/ml; Peprotech). In some experiments, cells obtained at the indicated days of the NKT-ES/OP9/Dll-1 cultures were further cocultured on OP9/control. The method outlined above is similar to a published protocol (also see Supplemental Figure 3) (30).

Quantitative real-time PCR. Total RNA was isolated from FACS-purified cell populations using the TRIzol reagent (Invitrogen). cDNA was prepared by Superscript III RNase H⁻ Reverse Transcriptase with random hexamers (Invitrogen). Quantitative real-time PCR was performed with SYBR GreenER qPCR SuperMix (Invitrogen) for ABI PRISM 7900HT (Applied Biosystems). Cells (2×10^3) for *Zbtb16*, *Sh2d1a*, or *Hprt* were used as templates. Gene-specific primer sequences were as follows: *Zbtb16*-fw: AACGGTTCCTGGACAGTTTG, *Zbtb16*-rv: CCCACACAGCAGACAGAAGA; *Sh2d1a*-fw: ACGCCTCTGCAGTATCCAGT, *Sh2d1a*-rv: ATGGTGCATTCAGGCAGATA; and *Hprt*-fw: TCCTCCTCAGACCGCTTTT, *Hprt*-rv: CCTGGTTCATCATCGCTAATC. Quantitative analysis was performed by ΔΔCt method by using *hprt* as an internal control.

Intracellular cytokine staining. Intracellular cytokine staining was performed as described previously (31). For IFN-γ staining in NKT cells and NK cells, liver MNCs from *Jα18*$^{-/-}$ mice that had received iPSC-derived NKT cells were prepared 16 hours after administration of α-GalCer. Brefeldin A (Sigma-Aldrich) was added for the last 4 to 5 hours of culture of liver MNCs to accumulate intracellular cytokines. Cells were then washed and incubated with α-GalCer/CD1d dimer and anti-mouse TCR-β mAb for NKT cells and anti-mouse NK1.1 and anti-mouse TCR-β mAb for NK cells for 20 minutes at 4°C after first blocking Fc receptors with an anti-CD16/CD32 antibody. Following fixation with Cytofix/Cytoperm Plus (BD Biosciences), cells were stained for intracellular IFN-γ for 15 minutes at room temperature.

T cell immunity. The experimental protocols for evaluating T cell immunity have been previously described in detail (see also Supplemental Figure 7 and ref. 5). Briefly, to prepare the cell-associated OVA, spleen cells from *TAP*$^{-/-}$ mice were treated with hypertonic medium in the presence of 10 mg/ml OVA and then incubated with hypotonic medium. The cell-associated form of OVA (2×10^7 cells/mouse) and 2 μg α-GalCer were coadministered i.v. to mice. Seven days later, spleen cells from immunized mice were cultured for 6 hours with 1 μM $OVA_{257\text{-}264}$ peptide in the presence of brefeldin A to accumulate IFN-γ intracellularly. Cells were incubated with the 2.4G2 mAb, then FITC anti-CD8 for 20 minutes at room temperature, and then permeabilized and stained for PE-conjugated anti-IFN-γ (XMG1.2) mAb. For reconstitution in *Jα18*$^{-/-}$ mice, iPSC-derived NKT cells (7a-NKT or 7g-NKT cells; 4×10^6 cells per mouse) were transferred i.v. Two weeks later, the mice were immunized with cell-associated OVA together with α-GalCer (TOG). A week later, spleen cells from the recipient mice were challenged with $OVA_{257\text{-}264}$ peptide and analyzed for IFN-γ production as above.

Tumor protection experiments. As above, 2×10^7 OVA-loaded spleen cells and 2 μg α-GalCer were coadministered to WT or *Jα18*$^{-/-}$ mice that had been transferred with 7a-NKT or 7g-NKT cells 2 weeks before. A week later, 2×10^5 EG7 cells were inoculated s.c. into the TOG-treated or naive mice. The parental non-OVA-transduced EL4 cells were used as control tumor cells. Tumor growth was monitored by measuring tumor size.

Statistics. The statistical significance of differences between the experimental groups was determined by the Mann-Whitney exact rank sum test. $P < 0.05$ was considered statistically significant.

Acknowledgments

The authors are grateful to P.D. Burrows for helpful comments and constructive criticism in the preparation of the manuscript.

Received for publication December 14, 2009, and accepted in revised form April 14, 2010.

Address correspondence to: Haruhiko Koseki, Laboratory for Developmental Genetics, RIKEN Research Center for Allergy and Immunology, Yokohama, Kanagawa 230-0045, Japan. Phone: 81.45.503.9689; Fax: 81.45.503.9688; E-mail: koseki@rcai.riken.jp. Or to: Masaru Taniguchi, Laboratory for Immune Regulation, RIKEN Research Center for Allergy and Immunology, Yokohama, Kanagawa 230-0045, Japan. Phone: 81.45.503.7001; Fax: 81.45.503.7003; E-mail: taniguti@rcai.riken.jp.

1. Taniguchi M, Harada M, Kojo S, Nakayama T, Wakao H. The regulatory role of Valpha14 NKT cells in innate and acquired immune response. *Annu Rev Immunol*. 2003;21:483–513.
2. Lantz O, Bendelac A. An invariant T cell receptor alpha chain is used by a unique subset of major histocompatibility complex class I-specific CD4⁺ and CD4⁻8⁻ T cells in mice and humans. *J Exp Med*. 1994;180(3):1097–1106.
3. Exley M, Garcia J, Balk SP, Porcelli S. Requirements for CD1d recognition by human invariant Valpha24⁺ CD4⁻CD8⁻ T cells. *J Exp Med*. 1997;186(1):109–120.
4. Fujii S, Shimizu K, Hemmi H, Steinman RM. Innate Valpha14(+) natural killer T cells mature dendritic cells, leading to strong adaptive immunity. *Immunol Rev*. 2007;220:183–198.
5. Cui J, et al. Requirement for Valpha14 NKT cells in IL-12-mediated rejection of tumors. *Science*. 1997; 278(5343):1623–1626.
6. Terabe M, Berzofsky JA. The role of NKT cells in tumor immunity. *Adv Cancer Res*. 2008;101:277–348.
7. Dhodapkar MV. Harnessing human CD1d restricted T cells for tumor immunity: progress and challenges. *Front Biosci*. 2009;14:796–807.
8. Okai M, et al. Human peripheral blood Valpha24+ Vbeta11+ NKT cells expand following administra-

tion of alpha-galactosylceramide-pulsed dendritic cells. *Vox Sang.* 2002;83(3):250–253.
9. Nieda M, et al. Therapeutic activation of Valpha24$^+$Vbeta11$^+$ NKT cells in human subjects results in highly coordinated secondary activation of acquired and innate immunity. *Blood.* 2004; 103(2):383–389.
10. Chang DH, et al. Sustained expansion of NKT cells and antigen-specific T cells after injection of alpha-galactosyl-ceramide loaded mature dendritic cells in cancer patients. *J Exp Med.* 2005;201(9):1503–1517.
11. Motohashi S, et al. A phase I-II study of alpha-galactosylceramide-pulsed IL-2/GM-CSF-cultured peripheral blood mononuclear cells in patients with advanced and recurrent non-small cell lung cancer. *J Immunol.* 2009;182(4):2492–2501.
12. Motohashi S, et al. A phase I study of in vitro expanded natural killer T cells in patients with advanced and recurrent non-small cell lung cancer. *Clin Cancer Res.* 2006;12(20 pt 1):6079–6086.
13. Watarai H, et al. Generation of functional NKT cells in vitro from embryonic stem cells bearing rearranged invariant V{alpha}14-J{alpha}18 TCR{alpha} gene. *Blood.* 2010;115(2):230–237.
14. Takahashi K, Yamanaka S. Induction of pluripotent stem cells from mouse embryonic and adult fibroblast cultures by defined factors. *Cell.* 2006;126(4):663–676.
15. Okita K, Ichisaka T, Yamanaka S. Generation of germline-competent induced pluripotent stem cells. *Nature.* 2007;448(7151):313–317.
16. Wernig M, et al. In vitro reprogramming of fibroblasts into a pluripotent ES-cell-like state. *Nature.* 2007;448(7151):318–324.
17. Savagem AK, et al. The transcription factor PLZF directs the effector program of the NKT cell lineage. *Immunity.* 2008;29(3):391–403.
18. Kovalovsky D, et al. The BTB-zinc finger transcriptional regulator PLZF controls the development of invariant natural killer T cell effector functions. *Nat Immunol.* 2008;9(9):1055–1064.
19. Nichols KE, et al. Regulation of NKT cell development by SAP, the protein defective in XLP. *Nat Med.* 2005;11(3):340–345.
20. Pasquier B, et al. Defective NKT cell development in mice and humans lacking the adapter SAP, the X-linked lymphoproliferative syndrome gene product. *J Exp Med.* 2005;201(5):695–701.
21. Gonzalez-Aseguinolaza G, et al. Natural killer T cell ligand alpha-galactosylceramide enhances protective immunity induced by malaria vaccines. *J Exp Med.* 2002;195(5):617–624.
22. Fujii S, Shimizu K, Smith C, Bonifaz L, Steinman RM. Activation of natural killer T cells by alpha-galactosylceramide rapidly induces the full maturation of dendritic cells in vivo and thereby acts as an adjuvant for combined CD4 and CD8 T cell immunity to a coadministered protein. *J Exp Med.* 2003;198(2):267–279.
23. Hermans IF, et al. NKT cells enhance CD4+ and CD8+ T cell responses to soluble antigen in vivo through direct interaction with dendritic cells. *J Immunol.* 2003;171(10):5140–5147.
24. Fujii S, et al. Glycolipid alpha-C-galactosylceramide is a distinct inducer of dendritic cell function during innate and adaptive immune responses of mice. *Proc Natl Acad Sci U S A.* 2006;103(30):11252–11257.
25. Yamanaka S. Strategies and new developments in the generation of patient-specific pluripotent stem cells. *Cell Stem Cell.* 2007;1(1):39–49.
26. Hanna J, et al. Direct reprogramming of terminally differentiated mature B lymphocytes to pluripotency. *Cell.* 2008;133(2):250–264.
27. Hong H, et al. Suppression of induced pluripotent stem cell generation by the p53-p21 pathway. *Nature.* 2009;460(7259):1132–1135.
28. Osafune K, et al. Marked differences in differentiation propensity among human embryonic stem cell lines. *Nat Biotechnol.* 2008;26(3):313–315.
29. Bolstad BM, Collin F, Simpson KM, Irizarry RA, Speed TP. Experimental design and low-level analysis of microarray data. *Int Rev Neurobiol.* 2004; 60:25–58.
30. Cho SK, Zúñiga-Pflücker JC. Development of lymphoid lineages from embryonic stem cells in vitro. *Methods Enzymol.* 2003;365:158–169.
31. Watarai H, Nakagawa R, Omori-Miyake M, Dashtsoodol N, Taniguchi M. Methods for detection, isolation and culture of mouse and human invariant NKT cells. *Nat Protoc.* 2008;3(1):70–78.

Cell Stem Cell
Article

ESCs Require PRC2 to Direct the Successful Reprogramming of Differentiated Cells toward Pluripotency

Carlos F. Pereira,[1] Francesco M. Piccolo,[1] Tomomi Tsubouchi,[1] Stephan Sauer,[1] Natalie K. Ryan,[1] Ludovica Bruno,[1] David Landeira,[1] Joana Santos,[1] Ana Banito,[2] Jesus Gil,[2] Haruhiko Koseki,[3] Matthias Merkenschlager,[1] and Amanda G. Fisher[1,*]
[1]Lymphocyte Development Group
[2]Cell Proliferation Group
MRC Clinical Sciences Centre, Imperial College School of Medicine, Hammersmith Hospital, Du Cane Road, London W12 0NN, UK
[3]Department of Developmental Genetics, RIKEN Research Center for Allergy and Immunology, RIKEN Yokohama Institute, Yokohama, Japan
*Correspondence: amanda.fisher@csc.mrc.ac.uk
DOI 10.1016/j.stem.2010.04.013

SUMMARY

Embryonic stem cells (ESCs) are pluripotent, self-renewing, and have the ability to reprogram differentiated cell types to pluripotency upon cellular fusion. Polycomb-group (PcG) proteins are important for restraining the inappropriate expression of lineage-specifying factors in ESCs. To investigate whether PcG proteins are required for establishing, rather than maintaining, the pluripotent state, we compared the ability of wild-type, PRC1-, and PRC2-depleted ESCs to reprogram human lymphocytes. We show that ESCs lacking either PRC1 or PRC2 are unable to successfully reprogram B cells toward pluripotency. This defect is a direct consequence of the lack of PcG activity because it could be efficiently rescued by reconstituting PRC2 activity in PRC2-deficient ESCs. Surprisingly, the failure of PRC2-deficient ESCs to reprogram somatic cells is functionally dominant, demonstrating a critical requirement for PcG proteins in the chromatin-remodeling events required for the direct conversion of differentiated cells toward pluripotency.

INTRODUCTION

PcG proteins were originally identified in *Drosophila melanogaster* where they comprise multiprotein complexes required for maintaining the transcriptional silencing of a subset of repressed genes (reviewed in Ringrose and Paro, 2004). In recent years the biochemical properties of different Polycomb repressor complexes (PRCs) have been clarified in mammals and invertebrates, as has their genome-wide distribution (Boyer et al., 2006; Lee et al., 2006; Schwartz et al., 2006). This provided valuable insights into the mechanisms by which they repress transcription and convey cellular memory. Two main repressor complexes, PRC1 and PRC2, with different catalytic properties and core components have been identified. In mammals PRC2 activity depends on three core subunits, embryonic ectoderm development (Eed), suppressor of Zeste 12 (Suz12) and the SET domain-containing protein Enhancer of Zeste homolog 2 (Ezh2) that catalyzes histone H3 methylation at lysine 27 (reviewed in Simon and Kingston, 2009). PRC2-mediated H3K27me3 provides a docking site for PRC1 (Min et al., 2003), a multiprotein complex thought to be a direct executor of silencing. It contains four generic core components (Ring1A/Ring1B, Bmi1/Mel18, Ph1/2, and Pc1/2/3), and catalyzes histone H2A mono-ubiquitination of lysine 119 (reviewed in Simon and Kingston, 2009). PRC1-mediated silencing probably operates through a variety of mechanisms and there is evidence supporting PRC1 in the blocking of transcriptional elongation of RNA Polymerase II engaged at target sites (Stock et al., 2007), as well as in directing chromatin compaction (Francis et al., 2004). Studies in *Drosophila melanogaster* have also suggested that O-linked glycosylation, mediated by the PcG protein Sxc may also have a significant role in Polycomb repression (Gambetta et al., 2009; Sinclair et al., 2009).

We do not know the complete repertoire of roles played by PcG proteins in mammalian development. In human and mouse ESCs, PRC1 and PRC2 localize to the promoters of a subset of repressed genes encoding transcription factors required for specification later during development. These genes contain overlapping binding sites for the pluripotency-associated factors Oct4, Sox2, Nanog, and Sall4 within their promoters (Boyer et al., 2005, 2006; Lee et al., 2006; Yang et al., 2008) and are enriched for both histone H3K4me3 and H3K27me3 (Azuara et al., 2006; Bernstein et al., 2006). Withdrawal of PRC1 or PRC2 activity from mouse ESCs results in global gene derepression of these target genes (Azuara et al., 2006; Boyer et al., 2006; Jorgensen et al., 2006; Lee et al., 2006) and unscheduled differentiation (Boyer et al., 2006; Endoh et al., 2008), consistent with PRCs being important for maintaining pluripotency. Furthermore, Ezh2-deficient embryos die early in gestation and *null* blastocysts fail to generate ESC lines (O'Carroll et al., 2001), so PRC2 may also be critical for establishing pluripotency. To investigate this, we have taken advantage of the documented capacity of ESCs to directly reprogram differentiated somatic cells to pluripotency in experimental heterokaryons (Pereira and Fisher, 2009; Pereira et al., 2008). Previous studies with

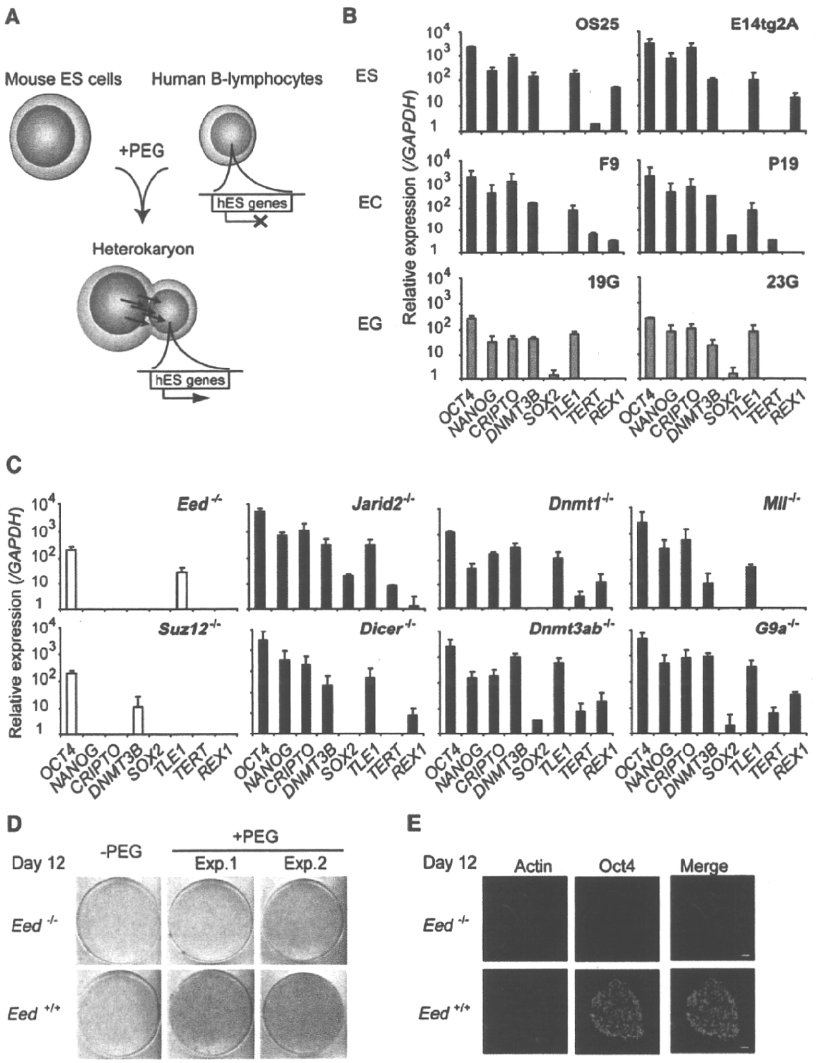

Figure 1. Heterokaryon Reprogramming of Human B Lymphocytes to Pluripotency by Mouse ESCs, ECCs, and EGCs but Not ESCs Lacking either Eed or Suz12

(A) Schematic representation of the strategy for generating interspecies heterokaryons between human B lymphocytes and mouse ESCs.

(B) Reprogramming was evaluated by measuring the induction of human embryonic genes (*OCT4*, *NANOG*, *CRIPTO*, *DNMT3B*, *SOX2*, *TLE1*, *TERT*, and *REX1*) from human-derived nuclei, via qRT-PCR and human gene-specific primers, 3 days after cell fusion. The reprogramming potential of mouse embryonic stem cells (ESCs, OS25 and E14tg2A cell lines, black bars), embryonic carcinoma cells (ECCs, F9 and P19 cell lines, dark gray bars), and embryonic germ cells (EGCs, 19G and 23G cell lines, light gray bars) is shown. Error bars indicate the SD of three independent experiments.

(C) qRT-PCR analysis of heterokaryons generated between human B lymphocytes and mouse ESCs knockout for the PRC2 members Eed and Suz12 (white bars), Jarid2, Dnmt1, Dnmt3a/b, Mll, G9a, and Dicer (black bars). Data were normalized to human *GAPDH* expression. Error bars indicate the SD of 2–3 independent experiments.

(D) Alkaline phosphatase staining of hybrid colonies obtained from fusions of puromycin-resistant mouse B cells with either Eed-deficient ($Eed^{-/-}$) or wild-type ($Eed^{+/+}$) ESCs. Fused cells (+PEG) or unfused controls (−PEG) were plated on puromycin-resistant feeder cells in ESC medium supplemented with puromycin for 12 days and stained for alkaline phosphatase activity. Average number of colonies from three experiments: $Eed^{-/-}$ × mouse B (23 ± 11), $Eed^{+/+}$ × mouse B (1945 ± 998).

(E) Oct4 expression, detected by immunofluorescence labeling (green), is retained by hybrid clones generated from fusing $Eed^{+/+}$ ESCs with mouse B cells, but is not expressed by hybrid clones generated from fusing $Eed^{-/-}$ ESCs with mouse B cells. Actin (red) staining is shown as a control. Scale bars represent 50 μm.

See also Figure S1 and Table S1.

this approach showed that the ability of ESCs to successfully reprogram somatic cells requires the expression of Oct4 (Pereira et al., 2008), a factor that is required for induced pluripotent stem cell (iPSC)-based reprogramming (Takahashi and Yamanaka, 2006; Yamanaka, 2009). Here, we show that mouse ESC lines conditionally depleted of PRC1 or PRC2 components fail to reprogram human B cells within heterokaryons, being unable to induce the successful remodeling of differentiated nuclei. This defective reprogramming is functionally dominant over wild-type, implying that misexpression of PRC target genes by ESCs actively interferes with their reprogramming capacity.

RESULTS

Human B Lymphocytes Are Reprogrammed by Mouse ESCs, ECCs, and EGCs

Heterokaryon assays in which human differentiated cells are reprogrammed by mouse ESCs have been used to study successful reprogramming and to define the factors required for this dominant conversion (Blau et al., 1985; Tada et al., 2001; Terranova et al., 2006). When fused with human B lymphocytes, mouse ESCs rapidly induce the expression of human pluripotency-associated genes (Pereira et al., 2008). Conversion requires mouse Oct4 (Pereira et al., 2008) and studies in hybrids suggest that ESCs share this property with other Oct4-expressing embryonic stem cells including embryonic carcinoma (EC, such as F9, P19) and embryonic germ (EG, such as 19G and 23G) cell lines (Do et al., 2007; Tada et al., 1997, 2001). Here, successful reprogramming was judged by qRT-PCR with primers selective for human *OCT4*, *NANOG*, *CRIPTO*, *DNMT3B*, *SOX2*, *TLE1*, *TERT*, and *REX1*, and expression was monitored from 0 to 3 days after cell fusion (Figures 1A and 1B; Figures S1A and S1B). Each of the ESC, ECC, and EGC lines induced pluripotency-associated gene expression by human B cells, albeit with slight variation (Figure 1B, middle and lower panels). For example, fusion of B lymphocytes with P19 induced higher

levels of human *SOX2* expression (and less *REX1*) than with F9, OS25, and E14tg2A cells in keeping with the idea that P19 preferentially differentiate toward neuronal lineages (Jones-Villeneuve et al., 1983) and ECCs have a narrower range of lineage potential than ESCs (Chambers and Smith, 2004). Reprogramming by 19G and 23G EGCs (Tada et al., 1998) was generally less efficient (Figure 1B; Figure S1B) and induction of *TERT* and *REX1*, a gene that is downregulated upon mouse epiblast formation (Pelton et al., 2002), was not detected. No obvious correlation between the magnitude of gene expression by parental lines and the subsequent initiation of human genes in heterokaryons was evident (data not shown). These results suggested that although subtle differences in reprogramming reflect the developmental origin of individual lines, all pluripotent stem cell lines tested here shared the capacity to dominantly reprogram.

ESCs that Lack PRC2 Activity Fail to Efficiently Reprogram

To determine whether PRC2 activity is important for reprogramming, we fused human B cells to mouse ESC lines that lacked individual PRC2 components. Eed-deficient and Suz12-deficient ESC lines were unable to induce the expression of most human pluripotency-associated genes upon fusion with human lymphocytes (Figure 1C), in contrast to matched parental and heterozygous controls (Figures S1C–S1F). ESCs that lacked H3K27me2/me3 by virtue of loss of Eed (Figure S1C) or Suz12 (Figure S1E) induced the partial expression of human *OCT4* (and either *TLE1* or *DNMT3B*), but not other human pluripotency markers (Figure 1C; Figures S1D and S1F). To determine whether this failure of PRC2-deficient ESCs to efficiently reprogram human B cells reflects a specific requirement for PRC2-mediated repression, we tested the reprogramming capacity of ESCs deficient in either Jarid2 (a noncatalytic component of PRC2) (Landeira et al., 2010; Li et al., 2010; Pasini et al., 2010; Peng et al., 2009; Shen et al., 2009) or other chromatin-remodeling components (Figure 1C, middle and right panels; details in Table S1). ESCs genetically deficient for factors involved in DNA methylation (*Dnmt1*$^{-/-}$, *Dnmt3a/b*$^{-/-}$), histone 3 lysine 4 methylation (*Mll*$^{-/-}$), histone 3 lysine 9 methylation (*G9a*$^{-/-}$), RNA interference (*Dicer*$^{-/-}$), or that lacked Jarid2 (*Jarid2*$^{-/-}$), retained the ability to successfully reprogram human B cells at levels comparable with parental wild-type ESCs.

To confirm that Eed-deficient ESCs are unable to reprogram lymphocytes, we performed hybrid analysis. Mouse B cells (Puro^{R}) were fused to either wild-type or Eed-deficient ESCs and hybrids were cultured for 12 days in the presence of puromycin. Reprogrammed colonies, visualized by alkaline phosphatase staining, were abundant in fusions performed with *Eed*$^{+/+}$ ESCs but very rare in fusions with *Eed*$^{-/-}$ ESCs (Figure 1D), and these colonies failed to express Oct4 protein (Figure 1E; Figure S1G). Reprogramming by wild-type ESCs was confirmed by the re-expression of GFP in hybrids formed with mouse B cells carrying an *Oct4*-GFP transgene (Figure S1H). To test whether this defect is ESC specific, we fused wild-type mouse ESCs (*Hprt*$^{-/-}$) with either *Ezh2*$^{flx/flx}$ or *Ezh2*$^{-/-}$ T cells, and we cultured hybrids for 12 days in HAT-containing media. The number of reprogrammed colonies was similar with wild-type and Ezh2-deficient lymphocytes (26 versus 13, respectively) (Figure S1I), so our data suggest that ESCs selectively require PRC2 activity to induce pluripotent conversion of lymphocytes.

Conditional Loss of PRC2 or PRC1 Ablates the Dominant Reprogramming Capacity of ESCs

Because long-term growth of ESCs in the absence PRC2 results in inappropriate upregulation of many important transcription factors and may therefore result in additional (i.e., non-PRC2 targeted) changes, we confirmed these finding with ESC lines that are inducible *null* for the catalytic component of PRC2, Ezh2. ESCs were derived from conditional *Ezh2* knockout mice (Su et al., 2003). Clone Ezh2-1.3 carries a tamoxifen-inducible conditional *Ezh2* mutation on both endogenous alleles and is progressively depleted of Ezh2 protein after the addition of tamoxifen (Figure S2A). Loss of Ezh2 resulted in loss of H3K27me3 (and reduced H3K27me2/me1) at 96 hr after tamoxifen addition, without consequent changes in either ESC self-renew or the efficiency of PEG-mediated cell fusion (data not shown). The reprogramming capacity of Ezh2-depleted ESCs was severely impaired and several genes were either not induced (*NANOG, REX1, TERT*) or only partially induced (*CRIPTO, OCT4*) (Figure 2A, upper panel; Figure S2B). Long-term removal of Ezh2 (Δ/Δ) also resulted in compromised reprogramming, although low levels of human *NANOG*, *CRIPTO*, and *OCT4* transcripts were detected, consistent with reports that Ezh1 can compensate for Ezh2 deficiency (Shen et al., 2008). Interestingly, silencing of human lymphoid-specific genes (*CD19*, *CD45*, and *CD37*) was unaffected by Ezh2 depletion (Figure 2A, lower panel), suggesting that ESCs require PRC2 selectively for activating pluripotency-associated genes during reprogramming.

To test whether the PRC1 activity was also required for reprogramming, we examined ESCs that were conditional *null* for Ring1A/B. Clone ES-ERT2 is homozygous *null* for the PRC1 component *Ring1A* and carries two tamoxifen-inducible conditional knockout *Ring1B* alleles. Accordingly, after tamoxifen addition, ES-ERT2 cells display a global reduction in H2A ubiquitylation and Ring1B expression, while overall levels of PRC2 proteins and trimethylated H3K27 remain largely unaffected (Endoh et al., 2008; Stock et al., 2007). ESCs lacking PRC1 did not successfully reprogram human B cells. As shown in Figure 2B and Figure S2C, tamoxifen pretreatment of ES-ERT2 cells resulted in the failure to induce *REX1* and *TERT* and impaired induction of *NANOG* and *CRIPTO*, although silencing of human lymphoid genes was again unaffected.

Reconstitution of Eed in Eed-Deficient ESCs Restores Reprogramming Activity

To validate that the reprogramming capacity of ESCs was dependent on PRC1/2, we rescued *Eed null* ESCs (clone B1.3) by transfecting a 180 kb BAC clone carrying the entire *Eed* locus. As anticipated, wild-type ESCs and stable transfectants expressed Eed protein isoforms and H3K27me3 as detected by western blotting (clone B1.3BAC; Figure 3A). ESCs lacking Eed (B1.3Neo) or after Eed reconstitution (B1.3BAC) were separately fused to hB-lymphocytes and their reprogramming capacity compared. Restoration of *Eed* rescued the reprogramming capacity of ESCs (Figure 3B, compare solid and open bars; Figure S3).

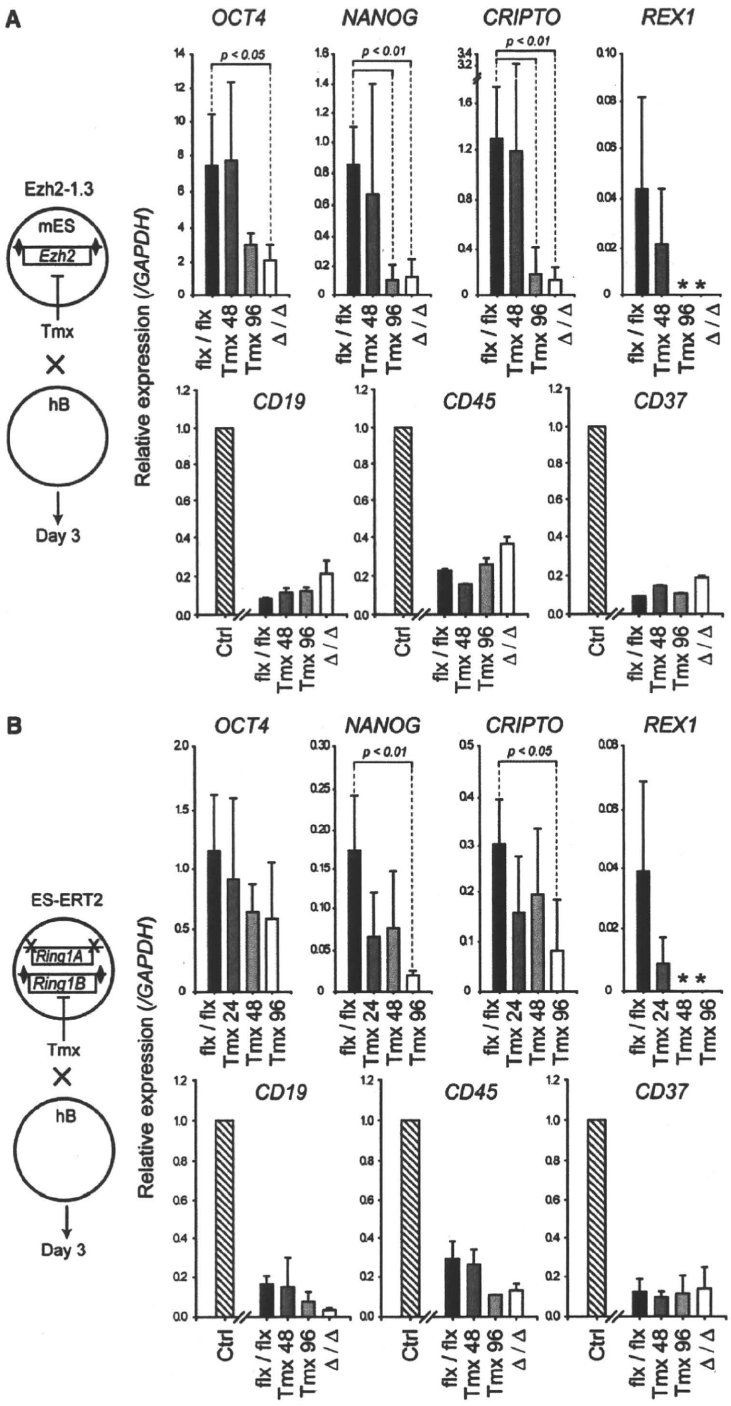

Figure 2. PRC2 or PRC1 Function Is Required for Reprogramming to Pluripotency

Ezh2-1.3 (A) and ES-ERT2 (B) cells containing the *Ezh2* and *Ring1B* conditional alleles, respectively, untreated (flx/flx, black bars) or treated with 800 nM tamoxifen for 24–96 hr (Tmx 24-96) were fused to human B lymphocytes. ESCs depleted long-term of *Ezh2* (Δ/Δ, white bars) were included as controls. Successful reprogramming was judged by the expression of human *OCT4*, *NANOG*, *CRIPTO*, and *REX1* transcripts, detected by qRT-PCR 3 days after cell fusion. Expression of human lymphocyte-specific genes (*CD19*, *CD45*, and *CD37*) declined after heterokaryon formation, as compared with levels before fusion (Ctrl). Data were normalized to human *GAPDH* expression. Error bars indicate the SD of four independent experiments. See also Figure S2.

Compromised Reprogramming by PRC2 Mutant ESCs Is Not due to a Deficit in Known Reprogramming Factors

To examine whether PRC2-deficient ESCs fail to efficiently reprogram human B cells because they misregulate endogenous factors that have previously shown to be critical for iPS-based reprogramming (Takahashi et al., 2007; Yu et al., 2007), we performed quantitative analyses of *Oct4*, *Nanog*, *Sox2*, *c-Myc*, *Klf4*, and *Lin28* in different PRC2 mutant ESC lines (Figure 4A). No major differences were detected in expression of these transcripts in ESCs lacking Eed, Suz12, and Ezh2, relative to matching wild-type controls. Nevertheless, as even slight variations in Oct4 are known to impact on ESC self-renewal, differentiation (Niwa et al., 2000), and reprogramming (Pereira et al., 2008), we engineered Eed-deficient ESC lines to modestly overexpress Oct4 by stable transfection of a Flag-tagged m*Oct4* transgene (B1.3-Oct4, clones 1D3 and 2D1, Figure 4B). Fusion of Oct4^{+}*Eed*$^{-/-}$ ESC lines did not rescue their capacity to reprogram human B cells (Figure 4C), in marked contrast to ESC lines that had been reconstituted with Eed (B1.3BAC1, B1.3BAC2). Thus, defective reprogramming is unlikely to be mediated by insufficient iPSC-inducing factors.

Dominant Reprogramming to Extraembryonic Lineages Is Not Induced by Eed-Deficient ESCs

Several developmental regulators are derepressed in ESCs that lack PRC2 activity and H3K27 methylation (Figure 5A; Azuara et al., 2006; Boyer et al., 2006; Lee et al., 2006), including the transcription factors Cdx2 and Hand1, that are required for the specification of trophectoderm (Rossant and Tam, 2009; Scott et al., 2000) and Gata6 and Hnf4, which are required for the development of primitive endoderm (Duncan et al., 1997; Rossant and Tam, 2009). We asked whether the misexpression of these factors by PRC2-deficient ESCs (Jorgensen et al., 2006) might result in dominant reprogramming to extraembryonic fates as stem cells derived from early blastocyst stages are know to be highly related (Santos et al., 2010). To test this possibility, we fused Eed-deficient ESCs with human lymphocytes and analyzed the induction of *CDX2*, *HAND1*, *GATA6*, and *HNF4* in the resulting heterokaryons. Whereas trophectoderm stem cells (TSCs) and extraembryonic endoderm (XEN) stem cells dominantly reprogrammed human B cells toward different extraembryonic lineages (inducing *CDX2/HAND1* or *GATA6/HNF4* expression,

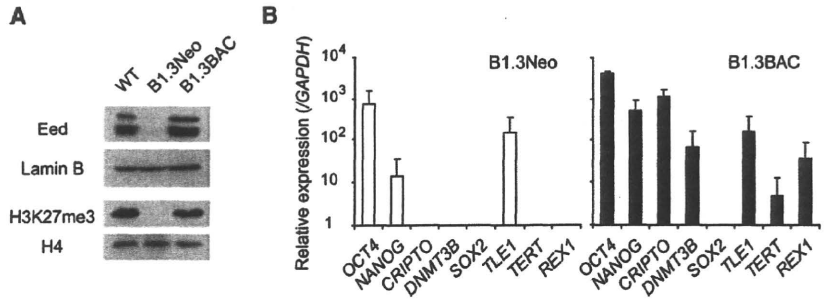

Figure 3. Reprogramming by Eed-Deficient ESCs Is Restored by Eed Rescue

(A) Eed-deficient B1.3 ESCs were rescued by insertion of a BAC clone that carried the *Eed* gene and neomycin resistance gene. Whole-cell lysates from these lines (B1.3BAC) and controls (B1.3Neo and WT ESCs) were analyzed by western blotting with antibodies to the Eed protein and anti-trimethylated histone 3 lysine 27 (H3K27me3). Equivalent protein loading is shown by Lamin B and total H4 detection.

(B) B1.3BAC and B1.3Neo ESCs were fused to human B lymphocytes and successful reprogramming was measured by activation of human embryonic genes 3 days after cell fusion. Data were normalized to human *GAPDH* expression. Error bars indicate the SD of 2–3 independent experiments. See also Figure S3.

respectively), PRC2-deficient ESCs failed to induce the correct expression of either set of markers (Figure 5B). These data suggest that PRC2-deficient ESCs do not reprogram human B cells toward an alternative, extraembryonic fate.

Eed-Deficient ESCs Display a Functionally Dominant Defect in Reprogramming

The compromised reprogramming capacity of Eed-deficient ESCs has at least two different interpretations. First, these ESCs could lack factors required for executing dominant conversion. Second, mutant ESCs may express factors that block the efficient reprogramming of differentiated cells. To distinguish between these possibilities, we generated heterokaryons that contained a human B cell nucleus, a wild-type mouse ESC nucleus, and an Eed-deficient ESC nucleus (Figure 5C) by prelabeling wild-type ESCs with DiI and $Eed^{-/-}$ ESCs with DiD. In brief, labeled cells were mixed in a 1:1 ratio with puromycin-resistant hB lymphocytes, fused with PEG, and cultured for

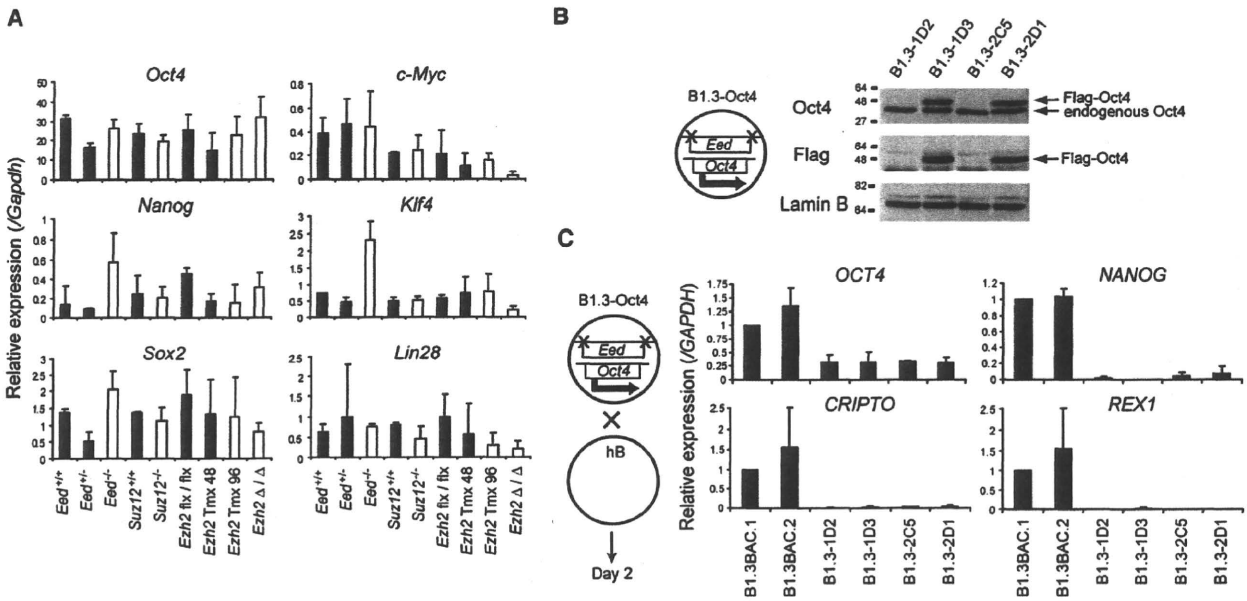

Figure 4. PRC2-Deficient ESCs Express Normal Levels of Reprogramming Factors

(A) Expression of mouse *Oct4*, *Nanog*, *Sox2*, *c-Myc*, *Klf4*, and *Lin28* transcripts by ESC lines deficient in PRC2 components (white); Eed ($Eed^{-/-}$), Suz12 ($Suz12^{-/-}$), Ezh2 (Tmx 96; $Ezh2^{\Delta/\Delta}$) versus their matched wild-type controls (black bars), analyzed by qRT-PCR. Data were normalized to mouse *Gapdh* expression and results shown are the mean and SD of three experiments.

(B) Western blotting of whole cell extracts of Eed-deficient ESCs (B1.3) and derived lines stably transfected with Oct4-Flag (clones 1D2, 1D3, 2C5, 2D1), with Oct4 or Flag antibodies. Transgene-derived Flag-Oct4 protein was detected in two clones (1D3 and 2D1) at levels similar to that of endogenous Oct4. Lamin B provides a control for protein loading. Approximate molecular sizes (in kD) are indicated.

(C) B1.3-Oct4 ESC clones were separately fused with human B cells and induction of human ESC-associated genes was monitored by qRT-PCR, 2 days after fusion. Eed-deficient ESCs transduced with an Eed containing BAC (clones B1.3BAC1 and B1.3BAC2) and Eed-deficient ESCs that do not express transgenic Oct4-Flag protein (clones B1.3-1D2 and B1.3-2C5) provided positive and negative controls for this analysis, respectively. Data were normalized to human *GAPDH* expression and results shown are the mean and SD of three independent experiments.

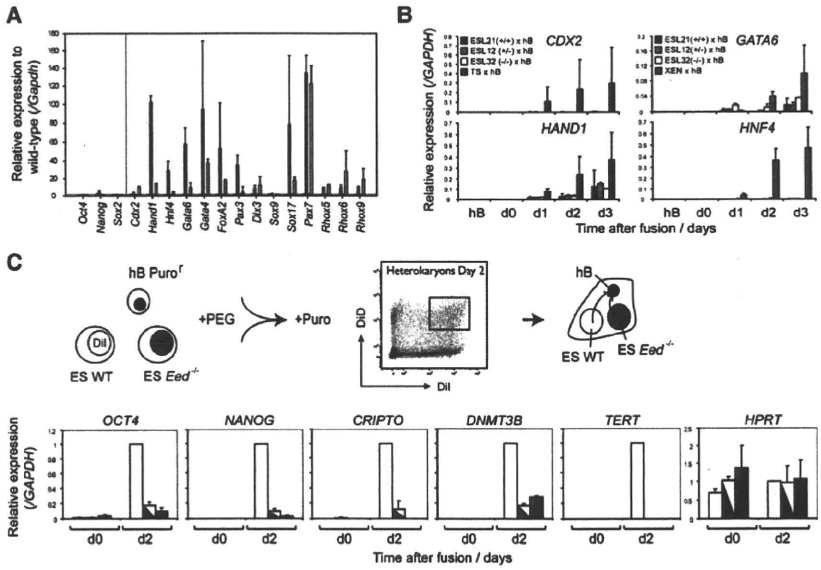

Figure 5. Defective Reprogramming of Human B Cells by Eed-Deficient ESCs Is Functionally Dominant

(A) Expression of developmental regulators is upregulated in mouse ESCs that lack either Eed (clone ESL32, red) or Suz12 (Suz12KO, white) relative to wild-type ESCs. Transcript abundance was estimated by qRT-PCR and is expressed as fold change of mutant versus matched wild-type control line (black). Expression of non-PRC2 target genes (*Oct4*, *Nanog*, *Sox2*) is shown as a control. Data were normalized to mouse *Gapdh* expression and the results are mean and SD of three experiments.

(B) The ability of Eed wild-type (ESL21, black), heterozygous (ESL12, gray), or homozygous *null* (ESL32, white) ESC lines to convert human B cells toward extraembryonic lineages was assessed by monitoring the induction of transcripts for human trophectoderm (*CDX2*, *HAND1*) and primitive endoderm (*GATA6*, *HNF4*) over a 3 day period after heterokaryon formation via qRT-PCR. Mouse trophectoderm stem (TS, blue) and primitive endoderm stem (XEN, green) cell lines were used as positive controls in the analysis. Data were normalized to human *GAPDH* expression and the results are mean and SD of two experiments.

(C) Strategy used to generate experimental trinucleate heterokaryons. Wild-type (ES WT) and Eed-deficient (ES Eed) cells were separately labeled with DiI or DiD membrane dyes, respectively, and fused with puromycin-resistant human B cells (hB Puro^r). 2 days after culture in puromycin, double (DiI/DiD) labeled heterokaryons were isolated by FACS sorting and successful reprogramming was estimated by qRT-PCR for the induction of human gene expression. Trinucleate heterokaryons containing pairs of wild-type ESCs (white) or pairs of *Eed*$^{-/-}$ ESCs (red) provide controls for this analysis. Data were normalized to human *GAPDH* expression and the results are mean and SD of three independent experiments. See also Figure S4.

2 days in the presence of puromycin, and dual-labeled heterokaryons were purified by FACS sorting. Successful reprogramming was judged by the induction of human *OCT4*, *NANOG*, *CRIPTO*, *DNMT3B*, *TLE1*, and *TERT* transcripts via quantitative RT-PCR. Heterokaryons containing Eed-deficient nuclei (red-white histogram, Figure 5C) expressed low levels of each of these genes as compared with fusions that contained either a single (not shown) or a pair of (open histogram, Figure 5C) wild-type nuclei. Mouse *Oct4, Nanog, Sox2, c-Myc, Klf4, Lin28* transcript expression was unaffected (Figure S4A) and served as a control in these experiments. These data argue that Eed-deficient ESCs do not simply lack factors required for reprogramming—because provision of a functionally competent (wild-type) nucleus did not restore reprogramming. Rather, Eed-deficient ESCs were functionally dominant over their wild-type counterparts, so PRC2 may be required to repress endogenous expression of genes that interfere with reprogramming. Attempts to define these PRC2 target genes examined 13 genes selected from transcriptome analyses of ESCs lacking Eed, Suz12, or Ezh2 (Figures S4B and S4C), but despite achieving efficient knockdown of candidate genes alone, or in combination, we were unable to fully restore reprogramming potential in Eed-deficient ESCs (Figure S4D).

Eed-Deficient ESCs Fail to Induce HP1α Redistribution and H3S10 Phosphorylation in Reprogrammed Lymphocytes

Previous studies have shown that reprogramming can result in profound changes in the nuclear volume and chromatin organization of differentiated nuclei (Pereira et al., 2008; Terranova et al., 2006). We examined whether PRC2-deficient ESCs induce similar changes in heterokaryons formed with human B cells. Mouse (ESC-derived) Oct4 protein was translocated into human nuclei with similar kinetics irrespective of whether wild-type or Eed-deficient ESCs were used as fusion partners (Figure 6A, arrow denotes human nuclei, and Table S2). We observed a rapid increase in nuclear size and changed architecture in human lymphocytes upon heterokaryon formation, to resemble human ESCs (Figures 6A and 6B). Eed-deficient ESCs induced similar changes in the volume (Figure 6B) and redistribution of nucleoli in lymphocyte-derived nuclei (Figure 6C; Figures S5A–S5C), as induced by wild-type controls. In contrast, Eed-deficient ESCs did not induce a redistribution of HP1α (from punctate to diffuse) and increased H3S10 phosphorylation, which are hallmark features of human ESCs and lymphocytes reprogrammed with wild-type ESCs (Figures 6D and 6E). Similar chromatin reorganization has recently been reported to occur upon reprogramming via nuclear transfer (Murata et al., 2010). HP1α recruitment is known to be modulated by Aurora B kinase-mediated phosphorylation of H3Ser10 (Fischle et al., 2003) and by JAK2 signaling (Dawson et al., 2009). Our data suggest a novel mechanistic link between these chromatin events and Eed-dependent reprogramming.

DISCUSSION

Here we show that ESCs, EGCs, and ECCs share the ability to efficiently reprogram human lymphocytes in heterokaryons and that this property is dependent on Polycomb repressor activity. The deletion of individual PRC1 or PRC2 members (Eed, Suz12, Ezh2, and Ring1A/B) that repress the expression of developmental regulators in ESCs abolishes the capacity of

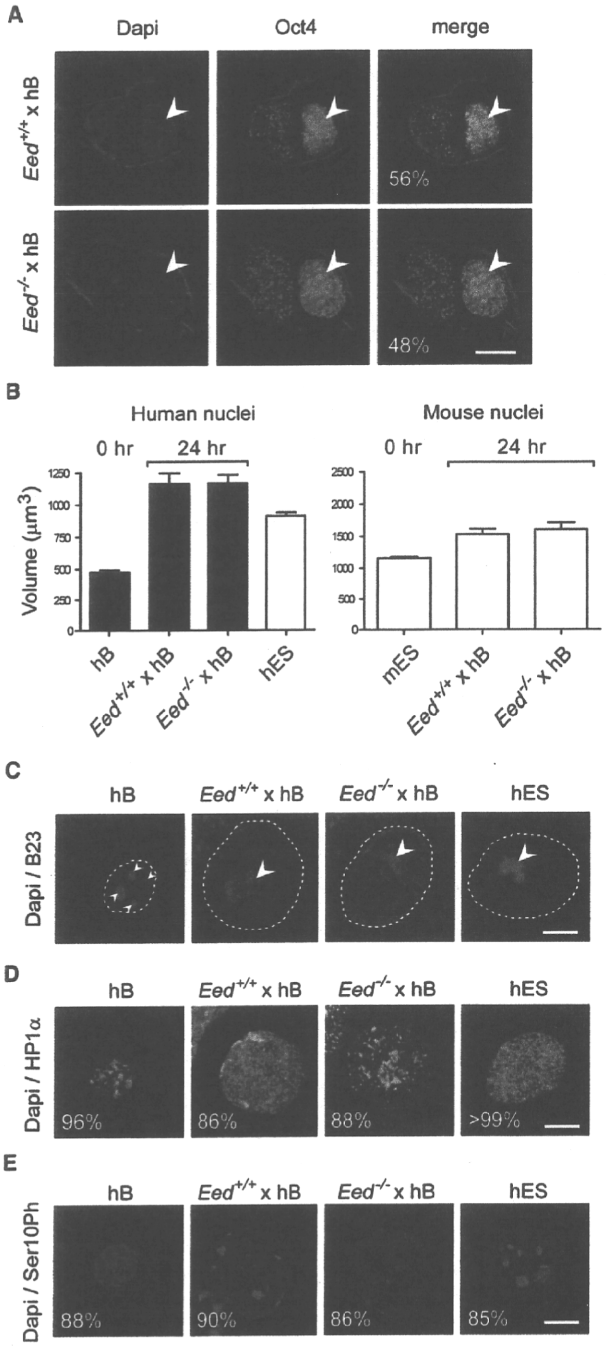

Figure 6. Impaired Chromatin Reorganization of Human B Cells Induced by Eed-Deficient ESCs

(A) ESC-derived Oct4 protein was detected (anti-Oct4, green) within human nuclei (arrows) 12 hr postfusion with mouse Eed-deficient ($Eed^{-/-}$) or wild-type ($Eed^{+/+}$) ESCs. Oct4 influx was detected in a similar proportion of human nuclei (percentage values shown in white) in both sets of heterokaryons. Human and mouse nuclei were distinguished on the basis of DAPI (blue) staining patterns (mouse punctate, human diffuse). Actin labeling (red) was used to delineate individual heterokaryons.

(B) The volume of human B cell (hB) nuclei before (0 hr) and 24 hr after (24 hr) heterokaryon formation with either Eed-deficient ($Eed^{-/-}$) or wild-type ($Eed^{+/+}$) ESCs was compared with human ESCs (hESC, H1 cell line). Nuclear volume was calculated as described in the Experimental Procedures, the volume of mouse nuclei before and after heterokaryon formation provides a control. Data shown are the mean and SD of 50–75 determinations per sample.

(C–E) The number of nucleoli (C), distribution of HP1α (D), and presence of H3S10ph (and H3K9me3) (E) within human B nuclei before (hB) and 24 hr after fusion with Eed-deficient or wild-type mouse ESCs was assessed by immunofluorescence via B23 antibody (red, nucleoli arrowed), anti-HP1α (green), and anti-H3S10ph/H3K9me3 (red). Human nuclei were identified via DAPI staining (blue) and are marked by a dashed line. Human ESCs (cell line H1) are shown as controls. Scale bars represent 10 μm. See also Figure S5 and Table S2.

ESCs to induce reprogramming. Eed-deficient mouse ESCs are themselves self-renewing, pluripotent, and can contribute to the three germ layers in vivo and in vitro (Chamberlain et al., 2008), so our data show that pluripotency and reprogramming function can be dissociated.

We demonstrate that Polycomb-mediated gene repression is critical for ESCs to actively convert differentiated cells to pluripotency. Surprisingly, defective reprogramming by PRC2-*null* ESCs was not restored in heterokaryons supplemented with wild-type ESC nuclei, showing that the reprogramming defect is functionally dominant. A requirement for PRC2 in reprogramming is consistent with previous studies in cloned mouse embryos (Zhang et al., 2009) and iPSCs (Mikkelsen et al., 2008), showing that failed or partially reprogrammed cells lack PRC2-dependent H3K27me3. Furthermore, recent iPSC studies with mouse lymphocytes and fibroblasts have suggested that inappropriate expression of some lineage-specific genes can impede reprogramming. For example, successful reprogramming of mouse B cells requires silencing of the B cell-specific factor Pax5 (Hanna et al., 2008; Xie et al., 2004). Reactivation or incomplete repression of lineage-specifying factors is also postulated to interfere with the establishment of core pluripotency networks because transient silencing of interfering factors significantly improves reprogramming efficiency (Mikkelsen et al., 2008). In this respect, reports that ESCs contain at least two types of bivalent domains (targeted by PRC2 only or by both PRC1 and PRC2) may be informative because PRC1-positive domains are enriched for genes encoding transcription factors that specify developmental fate (Ku et al., 2008). It is conceivable that repression of these targets in ESCs is particularly critical for reprogramming.

Interestingly, we show here that Jarid2-*null* ESCs are fully competent in reprogramming assays. Although these ESCs display variable levels of H3K27me3 (Li et al., 2010; Pasini et al., 2010; Peng et al., 2009; Shen et al., 2009), they do not show a genome-wide upregulation of PRC2 target genes (characteristic of Eed, Suz12, Ezh2, or Ring1A/B-depleted ESCs) and there is evidence that Jarid2 is not required for PRC2-mediated repression (Landeira et al., 2010). Taken together, our studies therefore suggest that pluripotent cells require active PcG-mediated repression of lineage-specifying factors to efficiently convey multilineage potential during reprogramming. Whether additional properties of PRC2, including the recruitment of RBP2 (H3K4 demethylase), to target genes in ESCs (Pasini et al., 2008) is important for reprogramming, awaits investigation.

In *Drosophila melanogaster,* downregulation of several PcG proteins occurs in regenerating leg disc cells and transdetermination of leg-to-wing is enhanced in PcG heterozygous mutant

flies (Lee et al., 2005). Downregulation of PcG proteins is also observed in regenerating skin in the mouse (Shaw and Martin, 2009), suggesting that reduced PcG protein levels may encourage lineage plasticity and enhance transdetermination (Lee et al., 2005; McClure et al., 2008). In view of these findings, it is possible that Polycomb proteins have different roles in undifferentiated versus somatic cells. Alternatively, the high "transcriptional noise" that results from global PcG-mediated gene derepression in ESCs (Chi and Bernstein, 2009) could be contributing to the poor reprogramming capacity of PRC2-*null* ESCs. However, this is unlikely to be the sole cause of the reprogramming defect because ESCs that lack Dicer, a factor that is critical for the global regulation of small RNAs (Cobb et al., 2005; Murchison et al., 2005), reprogram human B cells efficiently. Likewise, although recent studies have shown that the induction of senescence is a critical roadblock for successful reprogramming via iPS (reviewed in Krizhanovsky and Lowe, 2009), we show that levels of *p53*, *p21*, and *p16* are not appreciably changed when comparing wild-type or Eed-deficient ESCs or heterokaryons derived from them (Figure S5D) and that overexpression of p16 (a PRC2-target) by ESCs does not inhibit reprogramming (Figures S5E and S5F). This suggests that senescence induction is unlikely to be the cause of PRC2-*null* reprogramming defects.

In summary, here we show that Polycomb-mediated repression is required by mouse ESC lines to direct the conversion of differentiated cells toward pluripotency. ESCs lacking Eed induced rapid changes in the volume and architecture of differentiated human nuclei, but failed to direct the redistribution of HP1α, increased phosphorylation of H3S10, and to induce pluripotent gene expression that underlies successful reprogramming. Our results support the view that reprogramming is multistep and define Polycomb-dependent as well as Polycomb-independent events associated with the acquisition of a lineage-plastic state. Collectively, these studies show that the pluripotent and reprogramming capacities of ESCs can be mechanistically "uncoupled" and provided compelling new evidence that Polycomb-mediated gene repression is critical for establishing pluripotency.

EXPERIMENTAL PROCEDURES

Cell Culture

EBV-transformed hB clones were maintained in RPMI supplemented with 10% fetal calf serum (FCS, PAA Laboratories Gmbh, Pasching, Austria), 2 mM L-glutamine, and antibiotics (10 μg/ml penicillin and streptomycin). Abelson transformed mouse B cell lines were grown in RPMI supplemented with 20% FCS, nonessential amino acids, L-glutamine, 50 μM 2-mercaptoethanol, antibiotics, and IL-7 (5 ng/ml; R&D systems, Minneapolis, MN). Mouse ESC, EGC, and ECC lines were maintained on either irradiated mouse embryonic fibroblast (MEFs) feeder layers or 0.1% gelatin-coated surfaces with KO-DMEM medium,10% FCS, 5% knockout serum replacement (Invitrogen), nonessential amino acids, L-glutamine, 2-mercaptoethanol, antibiotics, and 1000 U/ml of leukemia inhibitory factor (ESGRO-LIF, Chemicon/Millipore). 4-hydroxy-tamoxifen (800 nM, Sigma) or puromycin (1 μg/ml, Sigma) was added to the cultures where indicated. Human ESC line H1 was cultured in medium conditioned by mitotically inactivated MEFs supplemented with 8 ng/ml bFGF (Peprotech, London, UK) on matrigel-coated plates, as previously described (Xu et al., 2001). Cells were routinely passaged at a 1:3 dilution by treatment with 200 U/ml collagenase IV (Invitrogen).

Generation of Transgenic Cell Lines

Eed-deficient ESCs (B1.3 clone) were transfected with a bacterial artificial chromosome (BAC, RP23-370F10), containing approximately 185 kb (nucleotides 97076839-97260535) of the forward DNA strand of mouse chromosome 7. In this clone, the chloramphenicol acetyltransferase (CAT) gene that was replaced with a neomycin resistance cassette from plasmid pL452 (NCI, Frederick, MD). B1.3-Oct4 ESC lines were generated by stable transfection of Flag-tagged mouse Oct4 in Eed-deficient ESCs (B1.3 clone). Mouse *Oct4* cDNA was cloned in the pDFLAG-cDNAIII vector (Invitrogen). The cDNA, including two flag sequences at the 5′ end, was excised and subcloned into a suitable vector for expression in ESCs (pCBA), with expression driven by the chicken β-actin promoter (Pereira et al., 2008). G418 selection (400 μg/ml; Invitrogen) was applied 48 hr after transfection and resistant clones were screened by western blot. Human and mouse B cells were transduced with a replication incompetent retroviral vector carrying a puromycin resistance gene and selected (1 μg/ml puromycin, Sigma) 48 hr after transfection.

Experimental Heterokaryons

Heterokaryons were generated by fusing mouse ESCs and human B lymphocytes with 50% polyethylene glycol (pH 7.4) (PEG 1500; Roche Diagnostics, Mannheim, Germany) as described previously (Pereira and Fisher, 2009). Mouse ESCs and hB lymphocytes were labeled with Vibrant 1,1′-dioctadecyl-3, 3, 3′, 3′ tetramethylindodicarbocyanine (DiD) and 1,1′-dioctadecyl-3, 3, 3′, 3′-tetramethylindocarbocyanine perchlorate (DiI) cell labeling solutions (Molecular Probes, Eugene, OR), respectively. Cells were resuspended at 1×10^6 cells/ml in DMEM and labeled with 5 μl/ml of dye at 37°C, 15 min. ESCs and hB were then mixed in a 1:1 ratio, washed, and fused with PEG (50%, at 37°C over 1 min before dilution). Cells were washed and cultured in ES media at 0.5×10^6 cells/cm^2. To eliminate unfused human B cells, Ouabain (10^{-5} M; Sigma) was added to the medium 4 hr after cell fusion. Proliferating ESCs were eliminated by the addition of 10^{-5} M Ara-C (Cytosine β-D arabino furanoside; Sigma) 4–6 hr after fusion and then removed after 16 hr. Trikaryons were generated by labeling Eed-deficient ESCs and wild-type ESCs with DiD and DiI, respectively, and mixing with Puro^R human B cells in 1:1:1 ratio, before cell fusion. Puromycin and Ouabain were added 6 hr after cell fusion to select for heterokaryons. After 2 days of culture, DiD$^+$DiI$^+$ cells were sorted and analyzed. For FACS analysis, a FACScalibur (BD Biosciences) with CellQuest software was used. FACS purification was performed with a FACSAria cell sorter.

Quantitative RT-PCR Analysis

RNA extraction was performed with RNA-BEE reagent (Tel-Test Inc., Friendswood, TX) and residual DNA was eliminated with the DNA-free kit (Ambion, Austin, TX). 3 μg of total RNA was then reverse transcribed with Superscript First-Strand Synthesis system (QIAGEN) with oligo $(dT)_{12\text{-}18}$ (Invitrogen). cDNAs of interest were then quantified with real-time qPCR amplification. Real-time PCR analysis was carried out on a Opticon DNA engine with Opticon Monitor software (MJ Research Inc., Waltham, MA), running the following program: 95°C for 15 min, then 40 cycles of 94°C for 15 s, 60°C for 30 s, 72°C for 30 s, followed by plate-read. PCR reactions included 2× Sybr-Green PCR Mastermix (QIAGEN), 300 nM primers, and 2 μl of template in a 35 μl reaction volume. Assays were performed in triplicate and data normalized according to *GAPDH* expression. Primers were designed with Primer Express software (Applied Biosystems) and pretested for the selective detection of human transcripts (and not mouse). Analysis of qPCR data was performed with the Opticon Monitor 3 software and the relative abundance of sequences was calculated with the ΔC(T) method (Pereira and Fisher, 2009).

Immunofluorescence and Western Blot Analysis

Immunofluorescence was performed as previously described (Terranova et al., 2006) with DAPI staining to distinguish mouse and human nuclei. Individual cells were delineated by F-actin staining (Phalloidin; A12380, Molecular Probes). Mouse monoclonal anti-Oct4 (611202; BD Biosciences, San Jose, CA), mouse monoclonal anti-HP1α antibody (MAB3584, Millipore, Lake Placid, NY), rabbit polyclonal anti-histone H3S10 phosphorylation (and H3K9me3) antibody (ab5819, Abcam, Cambridge, UK), and rabbit polyclonal anti-B23 (sc-5564; Santa Cruz Biotechnology Inc., Santa Cruz, CA) were used at 1:100 dilution. Secondary antibodies conjugated with fluorochromes were

purchased from Molecular Probes and used at 1:400 dilution. Samples were analyzed on a Leica TCS SP5 confocal microscope and processed with Leica software and Adobe Photoshop. To estimate nuclear volumes, *z*-stacks (0.5 μm distance) spanning individual nuclei were acquired. Volocity image processing software was used for 3D reconstructions and to quantify the nuclear volume. Nucleoli were discriminated on the basis of B23 labeling and counted in reconstructed projections. Western blot analysis was performed as previously described (Azuara et al., 2006) with goat polyclonal anti-Oct3/4 (sc-8628; Santa Cruz Biotechnology), mouse monoclonal anti-Flag (F3165, Sigma), mouse monoclonal anti-Eed (kindly provided by A. Otte, University of Amsterdam, The Netherlands), rabbit polyclonal anti-Suz12 (CS-029-050; Diagenode SA, Liège, Belgium), rabbit polyclonal anti-Ezh2 (CS-039-050; Diagenode), rabbit polyclonal anti-histone 3 lysine 27 monomethylation (07-448; Millipore), rabbit polyclonal anti-histone 3 lysine 27 dimethylation (07-452; Millipore), rabbit polyclonal anti-histone 4 lysine 20 trimethylation (07-463; Millipore). As loading controls, blots were incubated with anti-Lamin B goat polyclonal (sc-6216; Santa Cruz Biotechnology), rabbit polyclonal anti-histone 3 C terminus (ab1791; Abcam), and/or mouse monoclonal anti-histone 4 C terminus antibody (ab31827, Abcam). Each lane contained 20 μg total protein. For alkaline phosphate assays, hybrid colonies 12 days after cell fusion were stained with alkaline phosphatase assay kit.

Animal Procedures

Animals were housed and handled in accordance with the guidelines of the Imperial College subcommittee for animal research and the regulations set out by the British home office.

SUPPLEMENTAL INFORMATION

Supplemental Information includes five figures and two tables and can be found with this article online at doi:10.1016/j.stem.2010.04.013.

ACKNOWLEDGMENTS

We thank M. Casanova and N. Brockdorff for Eed-deficient ESC lines (ESL21, ESL12, and ESL32), T. Nesterova for Dicer-deficient ESC lines, E. Li for Dnmt1- and Dnmt3a/b-deficient ESCs, Y. Shinkai and T. Jenuwein for G9a-deficient ESCs, and M. Vidal for the *Ring1A*$^{-/-}$*Ring1B* conditional ESCs. We thank R. Lovell-Badge for F9 and P19 cell lines, A. Surani for the 19G and 23G cell lines, and J. Rossant for the TS and XEN cells used as controls. A. Surani and A. Tarakhovsky are thanked for Ezh2 conditional mice from which the conditional ESC lines were derived, A. Otte for the anti-Eed antibody, and S. Pinho, P. Noisa, and W. Cui for help with human ESC culture.

Received: September 21, 2009
Revised: March 5, 2010
Accepted: April 26, 2010
Published: June 3, 2010

REFERENCES

Azuara, V., Perry, P., Sauer, S., Spivakov, M., Jorgensen, H.F., John, R.M., Gouti, M., Casanova, M., Warnes, G., Merkenschlager, M., and Fisher, A.G. (2006). Chromatin signatures of pluripotent cell lines. Nat. Cell Biol. *8*, 532–538.

Bernstein, B.E., Mikkelsen, T.S., Xie, X., Kamal, M., Huebert, D.J., Cuff, J., Fry, B., Meissner, A., Wernig, M., Plath, K., et al. (2006). A bivalent chromatin structure marks key developmental genes in embryonic stem cells. Cell *125*, 315–326.

Blau, H.M., Pavlath, G.K., Hardeman, E.C., Chiu, C.P., Silberstein, L., Webster, S.G., Miller, S.C., and Webster, C. (1985). Plasticity of the differentiated state. Science *230*, 758–766.

Boyer, L.A., Lee, T.I., Cole, M.F., Johnstone, S.E., Levine, S.S., Zucker, J.P., Guenther, M.G., Kumar, R.M., Murray, H.L., Jenner, R.G., et al. (2005). Core transcriptional regulatory circuitry in human embryonic stem cells. Cell *122*, 947–956.

Boyer, L.A., Plath, K., Zeitlinger, J., Brambrink, T., Medeiros, L.A., Lee, T.I., Levine, S.S., Wernig, M., Tajonar, A., Ray, M.K., et al. (2006). Polycomb complexes repress developmental regulators in murine embryonic stem cells. Nature *441*, 349–353.

Chamberlain, S.J., Yee, D., and Magnuson, T. (2008). Polycomb repressive complex 2 is dispensable for maintenance of embryonic stem cell pluripotency. Stem Cells *26*, 1496–1505.

Chambers, I., and Smith, A. (2004). Self-renewal of teratocarcinoma and embryonic stem cells. Oncogene *23*, 7150–7160.

Chi, A.S., and Bernstein, B.E. (2009). Developmental biology. Pluripotent chromatin state. Science *323*, 220–221.

Cobb, B.S., Nesterova, T.B., Thompson, E., Hertweck, A., O'Connor, E., Godwin, J., Wilson, C.B., Brockdorff, N., Fisher, A.G., Smale, S.T., and Merkenschlager, M. (2005). T cell lineage choice and differentiation in the absence of the RNase III enzyme Dicer. J. Exp. Med. *201*, 1367–1373.

Dawson, M.A., Bannister, A.J., Gottgens, B., Foster, S.D., Bartke, T., Green, A.R., and Kouzarides, T. (2009). JAK2 phosphorylates histone H3Y41 and excludes HP1alpha from chromatin. Nature *461*, 819–822.

Do, J.T., Han, D.W., Gentile, L., Sobek-Klocke, I., Stehling, M., Lee, H.T., and Scholer, H.R. (2007). Erasure of cellular memory by fusion with pluripotent cells. Stem Cells *25*, 1013–1020.

Duncan, S.A., Nagy, A., and Chan, W. (1997). Murine gastrulation requires HNF-4 regulated gene expression in the visceral endoderm: Tetraploid rescue of Hnf-4(−/−) embryos. Development *124*, 279–287.

Endoh, M., Endo, T.A., Endoh, T., Fujimura, Y., Ohara, O., Toyoda, T., Otte, A.P., Okano, M., Brockdorff, N., Vidal, M., and Koseki, H. (2008). Polycomb group proteins Ring1A/B are functionally linked to the core transcriptional regulatory circuitry to maintain ES cell identity. Development *135*, 1513–1524.

Fischle, W., Wang, Y., Jacobs, S.A., Kim, Y., Allis, C.D., and Khorasanizadeh, S. (2003). Molecular basis for the discrimination of repressive methyl-lysine marks in histone H3 by Polycomb and HP1 chromodomains. Genes Dev. *17*, 1870–1881.

Francis, N.J., Kingston, R.E., and Woodcock, C.L. (2004). Chromatin compaction by a polycomb group protein complex. Science *306*, 1574–1577.

Gambetta, M.C., Oktaba, K., and Muller, J. (2009). Essential role of the glycosyltransferase sxc/Ogt in polycomb repression. Science *325*, 93–96.

Hanna, J., Markoulaki, S., Schorderet, P., Carey, B.W., Beard, C., Wernig, M., Creyghton, M.P., Steine, E.J., Cassady, J.P., Foreman, R., et al. (2008). Direct reprogramming of terminally differentiated mature B lymphocytes to pluripotency. Cell *133*, 250–264.

Jones-Villeneuve, E.M., Rudnicki, M.A., Harris, J.F., and McBurney, M.W. (1983). Retinoic acid-induced neural differentiation of embryonal carcinoma cells. Mol. Cell. Biol. *3*, 2271–2279.

Jorgensen, H.F., Giadrossi, S., Casanova, M., Endoh, M., Koseki, H., Brockdorff, N., and Fisher, A.G. (2006). Stem cells primed for action: Polycomb repressive complexes restrain the expression of lineage-specific regulators in embryonic stem cells. Cell Cycle *5*, 1411–1414.

Krizhanovsky, V., and Lowe, S.W. (2009). Stem cells: The promises and perils of p53. Nature *460*, 1085–1086.

Ku, M., Koche, R.P., Rheinbay, E., Mendenhall, E.M., Endoh, M., Mikkelsen, T.S., Presser, A., Nusbaum, C., Xie, X., Chi, A.S., et al. (2008). Genomewide analysis of PRC1 and PRC2 occupancy identifies two classes of bivalent domains. PLoS Genet. *4*, e1000242.

Landeira, D., Sauer, S., Poot, R., Dvorkina, M., Mazzarella, L., Jørgensen, H.F., Pereira, C.F., Leleu, M., Piccolo, F.M., Spivakov, M., et al. (2010). JARID2 is a PRC2 component in ES cells required for PRC1 and RNA Pol II recruitment at developmental regulator genes and multi-lineage differentiation. Nat. Cell Biol., in press.

Lee, N., Maurange, C., Ringrose, L., and Paro, R. (2005). Suppression of Polycomb group proteins by JNK signalling induces transdetermination in *Drosophila* imaginal discs. Nature *438*, 234–237.

Lee, T.I., Jenner, R.G., Boyer, L.A., Guenther, M.G., Levine, S.S., Kumar, R.M., Chevalier, B., Johnstone, S.E., Cole, M.F., Isono, K., et al. (2006). Control of developmental regulators by Polycomb in human embryonic stem cells. Cell *125*, 301–313.

Li, G., Margueron, R., Ku, M., Chambon, P., Bernstein, B.E., and Reinberg, D. (2010). Jarid2 and PRC2, partners in regulating gene expression. Genes Dev. *24*, 368–380.

McClure, K.D., Sustar, A., and Schubiger, G. (2008). Three genes control the timing, the site and the size of blastema formation in *Drosophila*. Dev. Biol. *319*, 68–77.

Mikkelsen, T.S., Hanna, J., Zhang, X., Ku, M., Wernig, M., Schorderet, P., Bernstein, B.E., Jaenisch, R., Lander, E.S., and Meissner, A. (2008). Dissecting direct reprogramming through integrative genomic analysis. Nature *454*, 49–55.

Min, J., Zhang, Y., and Xu, R.M. (2003). Structural basis for specific binding of Polycomb chromodomain to histone H3 methylated at Lys 27. Genes Dev. *17*, 1823–1828.

Murata, K., Kouzarides, T., Bannister, A.J., and Gurdon, J.B. (2010). Histone H3 lysine 4 methylation is associated with the transcriptional reprogramming efficiency of somatic nuclei by oocytes. Epigenetics Chromatin *3*, 4.

Murchison, E.P., Partridge, J.F., Tam, O.H., Cheloufi, S., and Hannon, G.J. (2005). Characterization of Dicer-deficient murine embryonic stem cells. Proc. Natl. Acad. Sci. USA *102*, 12135–12140.

Niwa, H., Miyazaki, J., and Smith, A.G. (2000). Quantitative expression of Oct-3/4 defines differentiation, dedifferentiation or self-renewal of ES cells. Nat. Genet. *24*, 372–376.

O'Carroll, D., Erhardt, S., Pagani, M., Barton, S.C., Surani, M.A., and Jenuwein, T. (2001). The polycomb-group gene Ezh2 is required for early mouse development. Mol. Cell. Biol. *21*, 4330–4336.

Pasini, D., Hansen, K.H., Christensen, J., Agger, K., Cloos, P.A., and Helin, K. (2008). Coordinated regulation of transcriptional repression by the RBP2 H3K4 demethylase and Polycomb-Repressive Complex 2. Genes Dev. *22*, 1345–1355.

Pasini, D., Cloos, P.A., Walfridsson, J., Olsson, L., Bukowski, J.P., Johansen, J.V., Bak, M., Tommerup, N., Rappsilber, J., and Helin, K. (2010). JARID2 regulates binding of the Polycomb repressive complex 2 to target genes in ES cells. Nature *464*, 306–310.

Pelton, T.A., Sharma, S., Schulz, T.C., Rathjen, J., and Rathjen, P.D. (2002). Transient pluripotent cell populations during primitive ectoderm formation: correlation of in vivo and in vitro pluripotent cell development. J. Cell Sci. *115*, 329–339.

Peng, J.C., Valouev, A., Swigut, T., Zhang, J., Zhao, Y., Sidow, A., and Wysocka, J. (2009). Jarid2/Jumonji coordinates control of PRC2 enzymatic activity and target gene occupancy in pluripotent cells. Cell *139*, 1290–1302.

Pereira, C.F., and Fisher, A.G. (2009). Heterokaryon-based reprogramming for pluripotency. Curr. Protoc. Stem Cell Biol. *Chapter 4*, Unit 4B 1.

Pereira, C.F., Terranova, R., Ryan, N.K., Santos, J., Morris, K.J., Cui, W., Merkenschlager, M., and Fisher, A.G. (2008). Heterokaryon-based reprogramming of human B lymphocytes for pluripotency requires Oct4 but not Sox2. PLoS Genet. *4*, e1000170.

Ringrose, L., and Paro, R. (2004). Epigenetic regulation of cellular memory by the Polycomb and Trithorax group proteins. Annu. Rev. Genet. *38*, 413–443.

Rossant, J., and Tam, P.P. (2009). Blastocyst lineage formation, early embryonic asymmetries and axis patterning in the mouse. Development *136*, 701–713.

Santos, J., Pereira, C.F., Di-Gregorio, A., Spruce, T., Alder, O., Rodriguez, T., Azuara, V., Merkenschlager, M., and Fisher, A.G. (2010). Differences in the epigenetic and reprogramming properties of pluripotent and extra-embryonic stem cells implicate chromatin remodelling as an important early event in the developing mouse embryo. Epigenetics Chromatin *3*, 1.

Schwartz, Y.B., Kahn, T.G., Nix, D.A., Li, X.Y., Bourgon, R., Biggin, M., and Pirrotta, V. (2006). Genome-wide analysis of Polycomb targets in *Drosophila melanogaster*. Nat. Genet. *38*, 700–705.

Scott, I.C., Anson-Cartwright, L., Riley, P., Reda, D., and Cross, J.C. (2000). The HAND1 basic helix-loop-helix transcription factor regulates trophoblast differentiation via multiple mechanisms. Mol. Cell. Biol. *20*, 530–541.

Shaw, T., and Martin, P. (2009). Epigenetic reprogramming during wound healing: Loss of polycomb-mediated silencing may enable upregulation of repair genes. EMBO Rep. *10*, 881–886.

Shen, X., Liu, Y., Hsu, Y.J., Fujiwara, Y., Kim, J., Mao, X., Yuan, G.C., and Orkin, S.H. (2008). EZH1 mediates methylation on histone H3 lysine 27 and complements EZH2 in maintaining stem cell identity and executing pluripotency. Mol. Cell *32*, 491–502.

Shen, X., Kim, W., Fujiwara, Y., Simon, M.D., Liu, Y., Mysliwiec, M.R., Yuan, G.C., Lee, Y., and Orkin, S.H. (2009). Jumonji modulates polycomb activity and self-renewal versus differentiation of stem cells. Cell *139*, 1303–1314.

Simon, J.A., and Kingston, R.E. (2009). Mechanisms of Polycomb gene silencing: Knowns and unknowns. Nat. Rev. Mol. Cell Biol. *10*, 697–708.

Sinclair, D.A., Syrzycka, M., Macauley, M.S., Rastgardani, T., Komljenovic, I., Vocadlo, D.J., Brock, H.W., and Honda, B.M. (2009). *Drosophila* O-GlcNAc transferase (OGT) is encoded by the Polycomb group (PcG) gene, super sex combs (sxc). Proc. Natl. Acad. Sci. USA *106*, 13427–13432.

Stock, J.K., Giadrossi, S., Casanova, M., Brookes, E., Vidal, M., Koseki, H., Brockdorff, N., Fisher, A.G., and Pombo, A. (2007). Ring1-mediated ubiquitination of H2A restrains poised RNA polymerase II at bivalent genes in mouse ES cells. Nat. Cell Biol. *9*, 1428–1435.

Su, I.H., Basavaraj, A., Krutchinsky, A.N., Hobert, O., Ullrich, A., Chait, B.T., and Tarakhovsky, A. (2003). Ezh2 controls B cell development through histone H3 methylation and Igh rearrangement. Nat. Immunol. *4*, 124–131.

Tada, M., Tada, T., Lefebvre, L., Barton, S.C., and Surani, M.A. (1997). Embryonic germ cells induce epigenetic reprogramming of somatic nucleus in hybrid cells. EMBO J. *16*, 6510–6520.

Tada, T., Tada, M., Hilton, K., Barton, S.C., Sado, T., Takagi, N., and Surani, M.A. (1998). Epigenotype switching of imprintable loci in embryonic germ cells. Dev. Genes Evol. *207*, 551–561.

Tada, M., Takahama, Y., Abe, K., Nakatsuji, N., and Tada, T. (2001). Nuclear reprogramming of somatic cells by in vitro hybridization with ES cells. Curr. Biol. *11*, 1553–1558.

Takahashi, K., and Yamanaka, S. (2006). Induction of pluripotent stem cells from mouse embryonic and adult fibroblast cultures by defined factors. Cell *126*, 663–676.

Takahashi, K., Tanabe, K., Ohnuki, M., Narita, M., Ichisaka, T., Tomoda, K., and Yamanaka, S. (2007). Induction of pluripotent stem cells from adult human fibroblasts by defined factors. Cell *131*, 861–872.

Terranova, R., Pereira, C.F., Du Roure, C., Merkenschlager, M., and Fisher, A.G. (2006). Acquisition and extinction of gene expression programs are separable events in heterokaryon reprogramming. J. Cell Sci. *119*, 2065–2072.

Xie, H., Ye, M., Feng, R., and Graf, T. (2004). Stepwise reprogramming of B cells into macrophages. Cell *117*, 663–676.

Xu, C., Inokuma, M.S., Denham, J., Golds, K., Kundu, P., Gold, J.D., and Carpenter, M.K. (2001). Feeder-free growth of undifferentiated human embryonic stem cells. Nat. Biotechnol. *19*, 971–974.

Yamanaka, S. (2009). Elite and stochastic models for induced pluripotent stem cell generation. Nature *460*, 49–52.

Yang, J., Chai, L., Fowles, T.C., Alipio, Z., Xu, D., Fink, L.M., Ward, D.C., and Ma, Y. (2008). Genome-wide analysis reveals Sall4 to be a major regulator of pluripotency in murine-embryonic stem cells. Proc. Natl. Acad. Sci. USA *105*, 19756–19761.

Yu, J., Vodyanik, M.A., Smuga-Otto, K., Antosiewicz-Bourget, J., Frane, J.L., Tian, S., Nie, J., Jonsdottir, G.A., Ruotti, V., Stewart, R., et al. (2007). Induced pluripotent stem cell lines derived from human somatic cells. Science *318*, 1917–1920.

Zhang, M., Wang, F., Kou, Z., Zhang, Y., and Gao, S. (2009). Defective chromatin structure in somatic cell cloned mouse embryos. J. Biol. Chem. *284*, 24981–24987.

OPEN ACCESS Freely available online

PLoS one

A Novel Zinc Finger Protein Zfp277 Mediates Transcriptional Repression of the *Ink4a/Arf* Locus through Polycomb Repressive Complex 1

Masamitsu Negishi[1,4], Atsunori Saraya[1,4], Shinobu Mochizuki[2], Kristian Helin[3], Haruhiko Koseki[2,4], Atsushi Iwama[1,4]*

1 Department of Cellular and Molecular Medicine, Graduate School of Medicine, Chiba University, Chiba, Japan, **2** RIKEN Research Center for Allergy and Immunology, Laboratory for Developmental Genetics, Yokohama, Japan, **3** Biotech Research and Innovation Centre (BRIC) and Centre for Epigenetics, University of Copenhagen, Copenhagen, Denmark, **4** JST, CREST, Tokyo, Japan

Abstract

Background: Polycomb group (PcG) proteins play a crucial role in cellular senescence as key transcriptional regulators of the *Ink4a/Arf* tumor suppressor gene locus. However, how PcG complexes target and contribute to stable gene silencing of the *Ink4a/Arf* locus remains little understood.

Methodology/Principal Findings: We examined the function of Zinc finger domain-containing protein 277 (Zfp277), a novel zinc finger protein that interacts with the PcG protein Bmi1. Zfp277 binds to the *Ink4a/Arf* locus in a Bmi1-independent manner and interacts with polycomb repressor complex (PRC) 1 through direct interaction with Bmi1. Loss of *Zfp277* in mouse embryonic fibroblasts (MEFs) caused dissociation of PcG proteins from the *Ink4a/Arf* locus, resulting in premature senescence associated with derepressed $p16^{Ink4a}$ and $p19^{Arf}$ expression. Levels of both Zfp277 and PcG proteins inversely correlated with those of reactive oxygen species (ROS) in senescing MEFs, but the treatment of $Zfp277^{-/-}$ MEFs with an antioxidant restored the binding of PRC2 but not PRC1 to the *Ink4a/Arf* locus. Notably, forced expression of *Bmi1* in $Zfp277^{-/-}$ MEFs did not restore the binding of Bmi1 to the *Ink4a/Arf* locus and failed to bypass cellular senescence. A *Zfp277* mutant that could not bind Bmi1 did not rescue $Zfp277^{-/-}$ MEFs from premature senescence.

Conclusions/Significance: Our findings implicate Zfp277 in the transcriptional regulation of the *Ink4a/Arf* locus and suggest that the interaction of Zfp277 with Bmi1 is essential for the recruitment of PRC1 to the *Ink4a/Arf* locus. Our findings also highlight dynamic regulation of both Zfp277 and PcG proteins by the oxidative stress pathways.

Citation: Negishi M, Saraya A, Mochizuki S, Helin K, Koseki H, et al. (2010) A Novel Zinc Finger Protein Zfp277 Mediates Transcriptional Repression of the *Ink4a/Arf* Locus through Polycomb Repressive Complex 1. PLoS ONE 5(8): e12373. doi:10.1371/journal.pone.0012373

Editor: Giacomo Cavalli, Centre National de la Recherche Scientifique, France

Received April 15, 2010; **Accepted** July 31, 2010; **Published** August 24, 2010

Funding: This work was supported in part by Grants-in-Aid for Scientific Research (#21390289) and for the Global COE Program (Global Center for Education and Research in Immune System Regulation and Treatment), MEXT, Japan, a Grant-in-Aid for the Core Research for Evolutional Science and Technology (CREST) from the Japan Science and Technology Corporation (JST), and a grant from the Takeda Science Foundation. The funders had no role in study design, data collection and analysis, decision to publish, or preparation of the manuscript.

Competing Interests: The authors have declared that no competing interests exist.

* E-mail: aiwama@faculty.chiba-u.jp

Introduction

Cellular senescence is a fundamental cellular program triggered after a finite number of cell divisions (replicative senescence) or more rapidly in response to acute stress (premature senescence). It functions as a cell-autonomous safeguard against severe genomic instability and carcinogenesis and contributes to aging in mammals as well. This irreversible cytostatic state can be triggered by multiple mechanisms, including telomere shortening, oxidative stress, cancer-causing genetic alterations, and DNA damage [1,2]. These intrinsic and extrinsic stress factors subsequently induce epigenetic derepression of the *Ink4a/Arf* tumor suppressor gene locus.

The *Ink4A/Arf* or *Cdkn2a* locus contains two distinct tumor suppressors, $p16^{Ink4}$ and $p19^{Arf}$ ($p14^{ARF}$ in humans) [3,4]. $p16^{Ink4a}$ protein directly inhibits the activities of the cyclin D-dependent kinases, Cdk4 and Cdk6, and maintains the pRb-E2f pathway in an anti-proliferative state, while $p19^{Arf}$ controls the stabilization and activation of p53 through binding to Mdm2, and promotes cellular senescence in primary fibroblasts [5]. Although both $p16^{Ink4a}$ and $p19^{Arf}$ play an important role in cellular mortality [6,7,8], there seem to be species-specific differences in their function. For example, the $p16^{INK4A}$-pRB-E2F pathway plays a major role in regulating the cellular senescence in human primary fibroblasts, whereas the $p19^{Arf}$-Mdm2-p53 pathway does so in MEFs [9,10].

PcG complexes are key regulators of epigenetic cellular memory. They establish and maintain cellular identities during embryogenesis, development, and tumorigenesis [11]. They have also been implicated in the maintenance of embryonic and somatic stem cells [12]. Among PcG proteins, Bmi1 and its role in the inheritance of the stemness of adult somatic stem cells have been well characterized [13,14]. One of the major targets of the PcGs, including Bmi1, is the *Ink4a/Arf* locus. Loss of *Bmi1* causes

derepression of the *Ink4a* and *Arf* genes, resulting in premature fibroblast senescence and depletion of hematopoietic and neural stem cells [13,14,15]. Conversely, forced expression of *Bmi1* extends the replicative life span of MEFs in tissue culture and enhances stem cell activity, at least partially, by repressing the *Ink4a/Arf* locus [16,17,18,19]. These observations indicate that PcG proteins are critical regulators of cellular senescence through the *Ink4a/Arf* locus.

Biochemical and genetic studies have identified that PcG complexes can be functionally separated into at least two distinct complexes: an initiation complex, PRC2, and a maintenance complex, PRC1. The human PRC2 core complex contains EZH2, EED, SUZ12, and RBAP48 (Nurf55 in *Drosophila*). PRC2 possesses catalytic activity specific for the trimethylation of histone H3 at lysine 27 (H3K27me3) and mono- and dimethylation of histone H1 at lysine 26 (H1K26me1/me2) [11,20,21]. The trimethylation of H3K27 is a repressive histone modification essential for gene silencing by PcGs and it has been suggested that this epigenetic mark functions to recruit PRC1 to chromatin [22]. By contrast, the PRC1 core complex contains RING2 (Ring1B in mice), BMI1, HPH, and CBX and possesses E3 ubiquitin ligase activity for the monoubiquitination of histone H2A at lysine 119 (H2AK119ub1) [21,23]. H2AK119ub1 has been suggested to play a central role in PRC1-mediated gene repression [24,25] and some data indicate that this modification interferes with translational elongation by restraining poised RNA polymerase II at bivalent genes in embryonic stem (ES) cells [26].

To understand the molecular mechanism of PcG gene silencing, we previously performed a yeast two-hybrid screening and identified a novel Bmi1-interacting protein, Zpf277 (known as ZNF277 in humans). In this study, we show that Zfp277 is required for the stable accumulation of PRC1 at the *Ink4a/Arf* locus and plays a critical role in the regulation of cellular senescence.

Results

Zfp277 binds to Bmi1 in mammalian cells

In a previously published yeast two-hybrid screening [27], we identified Zpf277 as a Bmi1-binding protein (data not shown). Mouse Zfp277 showed greater than 80% identity to human ZNF277 at the amino acid level and shared five highly conserved C_2H_2 zinc finger motifs (Figure. S1A). Human *ZNF277* was first documented as a gene located on chromosome 7 at q31 that is often deleted in several malignancies and autism [28,29]. Both mouse *Zfp277* and human *ZNF277* are ubiquitously expressed in a variety of tissues, including brain, heart, spleen, lung, and liver [28] (data not shown). However, the function of Zfp277 has not yet been described.

To confirm the physical interaction between Zfp277 and PcG proteins in mammalian cells, we conducted co-immunoprecipitation analyses of HA-tagged Zfp277 and Flag-tagged Bmi1, Ring1B, Ezh2, and Myc-tagged Mel18 using human 293T cells. As shown in Figure 1A, Zfp277 co-immunoprecipitated with Bmi1, but not with Ring1B or Ezh2. Of interest, Zfp277 did not co-immunoprecipitate with Mel18, another *Drosophila* Psc paralog in mammals which is 70% identical to Bmi1 at the amino acid level (Figure 1A). Next we employed a GST *in vitro* binding assay to confirm the physical interaction between Zfp277 and Bmi1 or Mel18 using GST-Bmi1 and GST-Zfp277, respectively. We confirmed that Zfp277 bound to Bmi1, but not to Mel18 (Figure 1B). Furthermore, endogenous PRC1 proteins, including Bmi1 and Ring1B, but not the PRC2 protein, Ezh2, were co-immunoprecipitated with Zfp277 using an anti-Zfp277 polyclonal antibody from the whole-cell lysate of MEFs (Figure 1C). Conversely, Zfp277 and Ring1B were co-immunoprecipitated with Bmi1 using an anti-Bmi1 antibody (Figure 1C). These findings suggested that Zfp277 interacts with PRC1 through direct binding to Bmi1, but not with PRC2.

Zfp277$^{-/-}$ MEFs undergo premature senescence

To explore the function of *Zfp277*, we generated *Zfp277* knockout mice (Figure S1B). Exon 5 and its flanking regions were replaced with a neomycin-resistance gene cassette by homologous recombination in ES cells. The presence of the *Zfp277* knockout allele was confirmed by Southern blot analysis (Figure S1C). Western blot analysis using an anti-Zfp277 polyclonal antibody also confirmed the absence of Zfp277 protein in *Zfp277*$^{-/-}$ MEFs (Figure S1D).

Zfp277$^{-/-}$ mice were born healthy and fertile (data not shown). Although detailed analyses of their phenotypes are underway, we found that *Zfp277*$^{-/-}$ MEFs from E12.5 embryos undergo premature senescence at early passages (Figure 1D). *Zfp277*$^{-/-}$ MEFs at passage 6 exhibited a flattened and enlarged appearance and were highly positive for senescence-associated β-galactosidase activity, a marker for cellular senescence (Figure S2). Expression of $p16^{Ink4a}$ and $p19^{Arf}$ was highly up-regulated in *Zfp277*$^{-/-}$ MEFs compared to their wild-type counterparts at early passages at both the mRNA and protein levels (Figure 1E and F). $p19^{Arf}$ reportedly plays a principal role in cellular senescence in mouse primary fibroblasts [9]. Correspondingly, premature senescence of *Zfp277*$^{-/-}$ MEFs was canceled by human papilloma virus-16 E6, which blocks the p19-Mdm2-p53 pathway [6] (Figure 1G), indicating that loss of *Zfp277* results in premature senescence of MEFs via the activation of the *Ink4a/Arf* locus.

Zfp277 binds to the *Ink4a/Arf* locus

Recent studies revealed that PcG proteins are downregulated and dissociate from the *Ink4a/Arf* locus when cells are exposed to intra- or extracellular stress, including tissue culture- and oncogene-induced stress [30–33]. To understand the functional crosstalk between Zfp277 and PcGs, we next tested if Zfp277 is associated with the *Ink4a/Arf* locus. Quantitative chromatin immunoprecipitation (Q-ChIP) assays were performed using antibodies specific for Zfp277, PcG proteins (Bmi1, Ring1B, Ezh2), and PcG histone modifications (H2AK119ub1 and H3K27me3) over the *Ink4a/Arf* locus in MEFs (Figure 2A and B). As demonstrated in Fig. 2B, Zfp277 as well as the PcG proteins and their histone modifications were broadly distributed across the *Ink4a/Arf* locus in presenescent MEFs. Notably, Zfp277 was dissociated from the *Ink4a/Arf* locus during serial passages like the PcG proteins and H3K27me3 (Figure 2C). In addition, the binding of PcG proteins and levels of H3K27 trimethylation exhibited a significant reduction throughout the *Ink4a/Arf* locus in *Zfp277*$^{-/-}$ MEFs to levels comparable to those in the wild-type MEFs at late passages (Figure 2B and C). These findings suggested that Zfp277 participates in the PcG-mediated gene silencing of the *Ink4a/Arf* locus.

Levels of Zfp277 and PcG proteins are regulated by oxidative stress

In general, culture-induced stress promotes the generation of reactive oxygen species (ROS), the main causative factor for oxidative stress. The balance between the generation and scavenging of ROS is critical for cellular senescence and organismal aging [10,34]. To assess whether oxidative stress affects the levels of Zfp277 and PcG proteins, we treated MEFs at

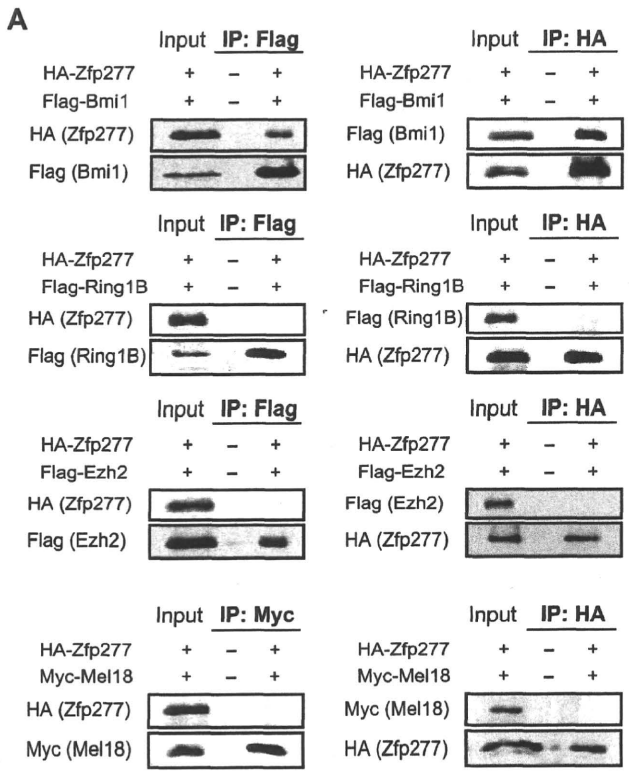
A
Input IP: Flag
HA-Zfp277 + – +
Flag-Bmi1 + – +
HA (Zfp277)
Flag (Bmi1)
Input IP: HA
HA-Zfp277 + – +
Flag-Bmi1 + – +
Flag (Bmi1)
HA (Zfp277)
Input IP: Flag
HA-Zfp277 + – +
Flag-Ring1B + – +
HA (Zfp277)
Flag (Ring1B)
Input IP: HA
HA-Zfp277 + – +
Flag-Ring1B + – +
Flag (Ring1B)
HA (Zfp277)
Input IP: Flag
HA-Zfp277 + – +
Flag-Ezh2 + – +
HA (Zfp277)
Flag (Ezh2)
Input IP: HA
HA-Zfp277 + – +
Flag-Ezh2 + – +
Flag (Ezh2)
HA (Zfp277)
Input IP: Myc
HA-Zfp277 + – +
Myc-Mel18 + – +
HA (Zfp277)
Myc (Mel18)
Input IP: HA
HA-Zfp277 + – +
Myc-Mel18 + – +
Myc (Mel18)
HA (Zfp277)

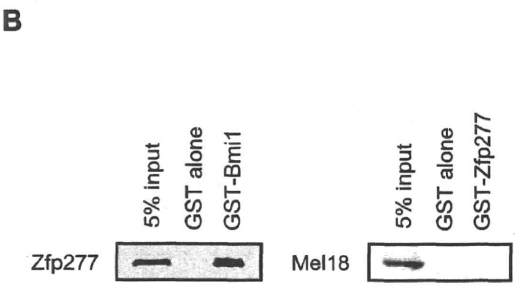
B
5% input
GST alone
GST-Bmi1
Zfp277
5% input
GST alone
GST-Zfp277
Mel18

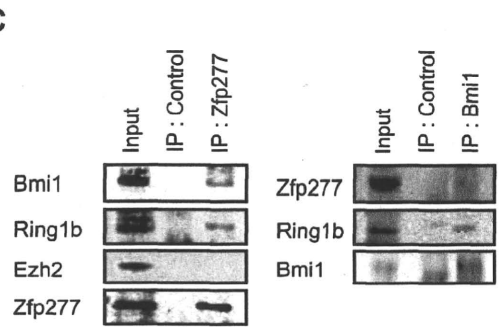
C
Input
IP : Control
IP : Zfp277
Bmi1
Ring1b
Ezh2
Zfp277
Input
IP : Control
IP : Bmi1
Zfp277
Ring1b
Bmi1

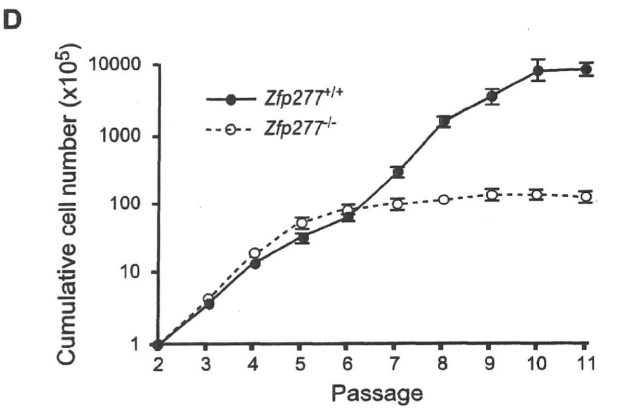
D
Cumulative cell number (x10^5)
10000
1000
100
10
1
Zfp277+/+
Zfp277-/-
2 3 4 5 6 7 8 9 10 11
Passage

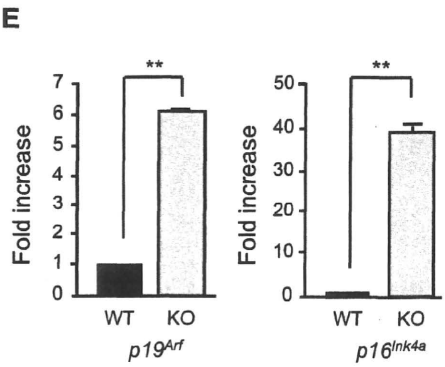
E
Fold increase
7
6
5
4
3
2
1
0
**
WT KO
p19Arf
Fold increase
50
40
30
20
10
0
**
WT KO
p16Ink4a

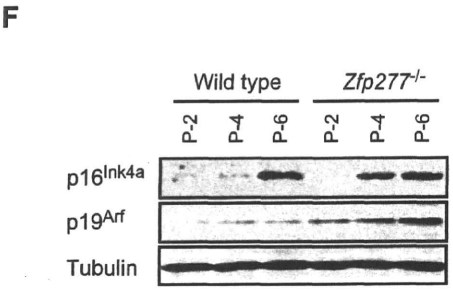
F
Wild type
Zfp277-/-
P-2
P-4
P-6
P-2
P-4
P-6
p16Ink4a
p19Arf
Tubulin

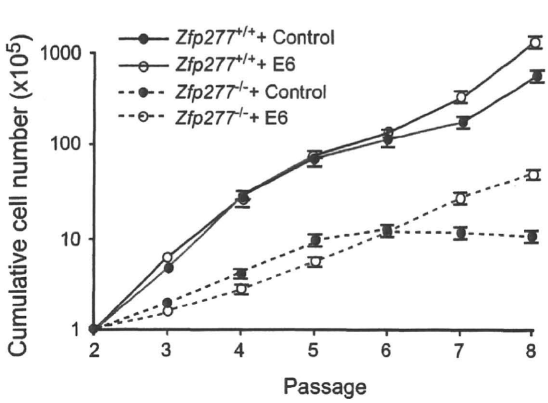
G
Cumulative cell number (x10^5)
1000
100
10
1
Zfp277+/+ + Control
Zfp277+/+ + E6
Zfp277-/- + Control
Zfp277-/- + E6
2 3 4 5 6 7 8
Passage

Figure 1. Zfp277 interacts physically with Bmi1. A. Zfp277 interacts with Bmi1 *in vivo*. HA-Zfp277 and Flag-tagged Bmi1, Ring1B, Ezh2, and Myc-tagged Mel18 were cotransfected into human 293T cells and the immunoprecipitates were subjected to a Western blot analysis using the antibodies indicated on the left. **B.** GST-pulldown between GST-Bmi1 and *in vitro*-translated Zfp277 (left panel) and GST-Zfp277 and *in vitro*-translated Mel18 (right panel). **C.** Binding of Zfp277 with PRC1 in MEFs. The whole-cell extracts from MEFs were immunoprecipitated with rabbit anti-Zfp277 serum (left panel) and anti-Bmi1 monoclonal antibody (right panel) or control IgG (control) and then subjected to Western blotting using the antibodies indicated on the left. A 2% input was loaded on the left. **D.** The growth curve of wild-type and *Zfp277*$^{-/-}$ MEFs. MEFs were seeded at 1×10^5 cells/well in 6-cm plates and replated at 1×10^5 cells/well every three days. Cumulative cell numbers are shown as the mean ± SD for three independent triplicate experiments. **E.** Quantitative RT-PCR analysis of *p19*^{Arf} and *p16*^{Ink4a} mRNA in MEFs at passage 2. mRNA levels were normalized to *Hprt1* expression. Expression levels relative to those in the wild-type MEFs are shown as the mean ± SD for three independent experiments. **F.** Expression of p19^{Arf} and p16^{Ink4a} in *Zfp277*$^{-/-}$ MEFs. The protein levels of p19^{Arf} and p16^{Ink4a} in wild-type and *Zfp277*$^{-/-}$ MEFs at the indicated passages were determined by Western blot analyses. Tubulin was used as a loading control. **G.** Rescue of the growth of *Zfp277*$^{-/-}$ MEFs by E6. Wild-type and *Zfp277*$^{-/-}$ MEFs were transduced with either a control or an *E6* retrovirus and cell growth was monitored every three days by replating at 1×10^5 cells/plate. Cumulative cell numbers are shown as the mean ± SD for three independent triplicate experiments. Statistical significance was determined with Student's t-test; $^{**}p<0.01$.
doi:10.1371/journal.pone.0012373.g001

an early passage (P-2) with hydrogen peroxide (H_2O_2) which induces the generation of ROS [35]. At 6 hrs after the treatment with H_2O_2 (100 μM), phosphorylation of Jnk, an indicator of activated oxidative stress pathways, was detected (Figure 3A). This treatment led to a significant reduction in Zfp277 and PcG protein (Bmi1, Mel18, Ring1B and Ezh2) levels. The level of H3K27 trimethylation also decreased. In contrast, expression of a histone H3K27 demethylase Jmjd3 was up-regulated (Figure 3A), consistent with previous results showing Jmjd3 expression to be induced in response to stress and oncogenic signaling [31]. Because *Zfp277*$^{-/-}$ MEFs undergo premature senescence, we next checked their levels of PcG proteins. As demonstrated in Figure 3B, they were decreased in *Zfp277*$^{-/-}$ MEFs compared to the passage-matched wild-type MEFs. As expected, the level of reactive oxygen species (ROS) was significantly higher in *Zfp277*$^{-/-}$ MEFs than the wild-type MEFs at the same passage (Figure S3), suggesting that the loss of Zfp277 leads to enhanced oxidative stress which could promote senescence.

An antioxidant, N-acetyl cysteine (NAC), counteracts oxidative stress and extends the replicative life span of primary fibroblasts [36]. NAC treatment increased the protein levels of Zfp277 as well as Bmi1, Ring1B, Mel18, and Ezh2 in wild-type MEFs (P-6) and of Bmi1 and Ezh2 even in *Zfp277*$^{-/-}$ MEFs (P-6) (Figure 3B). Furthermore, NAC treatment of wild-type and *Zfp277*$^{-/-}$ MEFs significantly repressed the expression of *p16*^{Ink4a} and *p19*^{Arf} (Figure 3C) and extended the cells' life span, although NAC itself had a mild adverse effect on proliferation as evident from the growth retardation of *Zfp277*$^{-/-}$ MEFs at early passages (Figure 3D). At passage 8, *Zfp277*$^{-/-}$ MEFs stopped growing and exhibited a flattened and enlarged appearance, while those treated with NAC kept growing and maintained a spindle-like shape (Figure 3E). These findings suggest Zfp277 as well as PcG proteins to be regulated by culture-associated oxidative stress in MEFs.

Levels of Zfp277 protein progressively declined during serial passaging, while the mRNA levels of *Zfp277* did not show any significant changes between MEFs at passages 2 and 6 (Figure 3F). Treatment of MEFs with the proteasome inhibitor MG132 remarkably restored levels of Zfp277 protein (Figure 3G). These findings indicate that the Zfp277 level is regulated by protein degradation in a proteasome-dependent manner.

Antioxidant treatment of *Zfp277*$^{-/-}$ MEFs restores the binding of PRC2 but not of PRC1 to the *Ink4a/Arf* locus

Antioxidant treatment downregulated the expression of *p19*^{Arf} in *Zfp277*$^{-/-}$ MEFs and extended the cells' life span during culture *ex vivo*. Therefore, we next tested whether antioxidant treatment can restore the binding of PcG proteins to the *Ink4a/Arf* locus in the absence of *Zfp277*. *Zfp277*$^{-/-}$ MEFs at very early passages (P-2) were treated with NAC and subjected to ChIP assays (Figure 4). NAC treatment successfully restored the binding of the PRC2 core protein Ezh2 and the amount of H3K27me3 to levels comparable to those in wild-type MEFs (P-1) (Figure 4F and H), while reducing the binding of Jmjd3 (Figure 4G). In striking contrast, the binding of Bmi1 was not restored at all and that of Ring1B was only mildly affected (Figure 4B and C). These findings clearly demonstrate that Zfp277 is required for PRC1 to localize to and repress the *Ink4a/Arf* locus and suggest that impaired binding of PRC1 to the *Ink4a/Arf* locus is the primary cause of the derepression which subsequently induces premature senescence in *Zfp277*$^{-/-}$ MEFs. Importantly, however, levels of H2A mono-ubiquitination moderately but significantly recovered in NAC-treated *Zfp277*$^{-/-}$ MEFs (Figure 4E) and the binding of Mel18 was restored to a level comparable to that in wild-type MEFs (P-1) (Figure 4D). Mel18 is a component of a PRC1-like complex capable of H2AK119 monoubiquitination and can functionally substitute for Bmi1 in many situations [37]. Thus, Zfp277 appears to crosstalk with Bmi1-containing PRC1 but not with the PRC1-like complex containing Mel18.

Forced expression of Bmi1 cannot bypass premature senescence of *Zfp277*$^{-/-}$ MEFs

Forced expression of Bmi1 in MEFs extends their life span through tight gene silencing of the *Ink4a/Arf* locus [16,38]. Therefore, we asked whether Bmi1 could extend the life span of *Zfp277*$^{-/-}$ MEFs. Forced expression of Bmi1 did not abrogate the premature senescence of *Zfp277*$^{-/-}$ MEFs at early passages (Figure 5A). Western blot analysis revealed that exogenous Bmi1 failed to repress the expression of p19^{Arf} (Figure 5B). Furthermore, ChIP analysis of Bmi1 demonstrated that the forced expression of Bmi1 only minimally promoted the binding of Bmi1 to the *Ink4a/Arf* locus in *Zfp277*$^{-/-}$ MEFs (P-2) (Figure 5C). These findings suggest that Zfp277 is required for recruitment of Bmi1 to or its stable accumulation at the *Ink4a/Arf locus* in MEFs.

Loss of Bmi1 does not affect the distribution of Zfp277 at the *Ink4a/Arf* locus

We next asked whether Bmi1 is required for the binding of Zfp277 to the *Ink4a/Arf* locus. *Bmi1*$^{-/-}$ MEFs undergo premature senescence (<P-6) [15] (Figure S4), and the generation of ROS is reportedly enhanced in the absence of Bmi1 [39]. So, we performed ChIP assays on *Bmi1*$^{-/-}$ MEFs cultured with or without NAC. ChIP analyses demonstrated that *Bmi1*-deficiency did not greatly affect the binding of Zfp277 to the *Ink4a/Arf* locus in early passage *Bmi1*$^{-/-}$ MEFs (Figure 6A). NAC treatment had a minimal effect on its binding. Binding of Ezh2 was not grossly altered, either (Figure 6F). In contrast, the binding of the PRC1 protein Ring1B and levels of histone modifications, H3K27me3

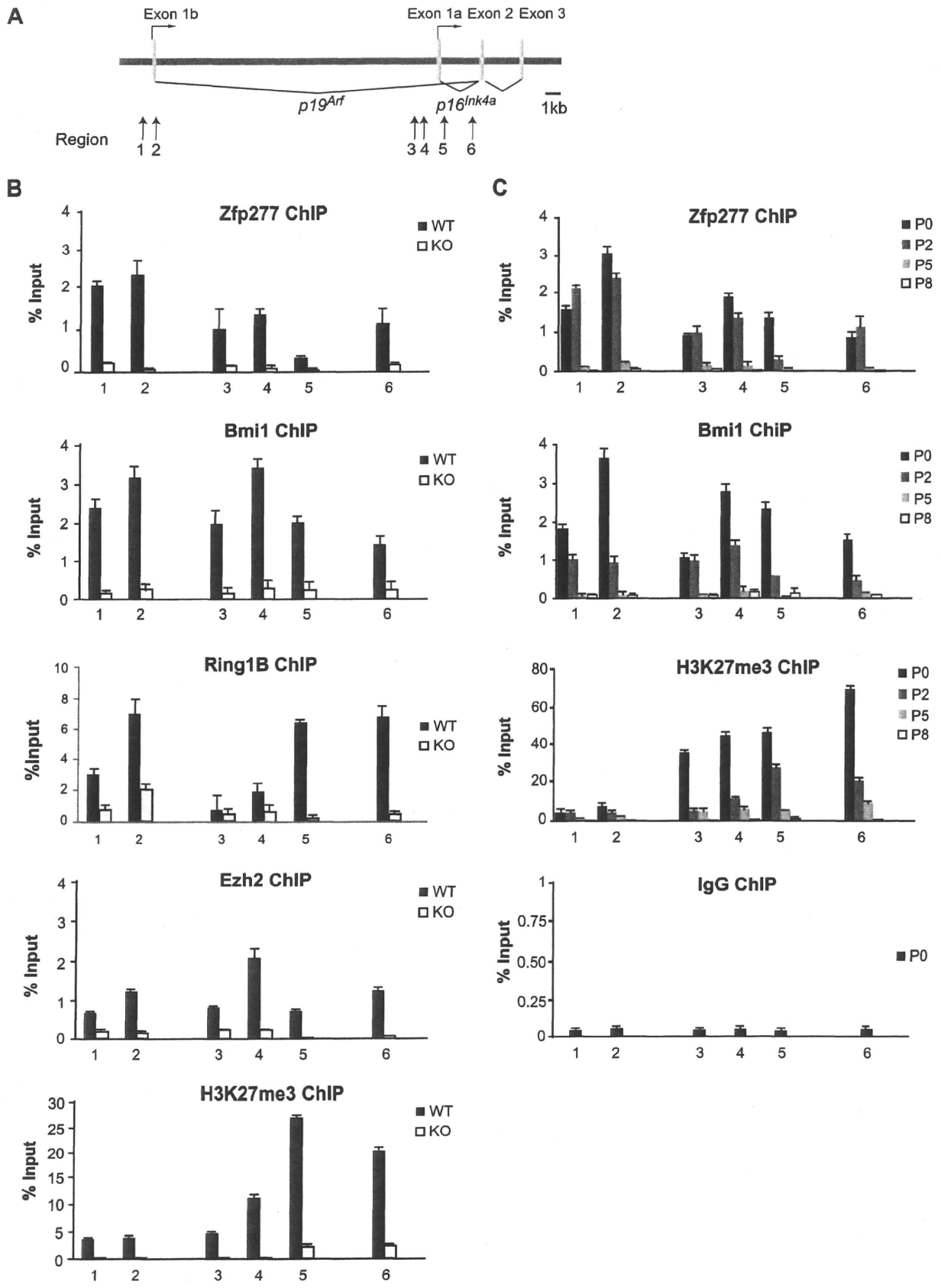
A
Exon 1b
Exon 1a Exon 2 Exon 3
p19Arf
p16Ink4a
1kb
Region
1 2
3 4 5 6
B
Zfp277 ChIP
Bmi1 ChIP
Ring1B ChIP
Ezh2 ChIP
H3K27me3 ChIP
% Input
%Input
WT
KO
C
Zfp277 ChIP
Bmi1 ChIP
H3K27me3 ChIP
IgG ChIP
% Input
P0
P2
P5
P8

Figure 2. Zfp277 binds the *Ink4a/Arf* locus and is downregulated during serial passaging. A. A schematic representation of the *Ink4a/Arf* locus. ChIP assays were performed using anti-Zfp277, Bmi1, Ring1B, Ezh2, and H3K27me3 antibodies. Regions amplified from the precipitated DNA by site-specific quantitative PCR are indicated by arrows. **B.** Q-ChIP analysis of the *Ink4a/Arf* locus in wild-type or *Zfp277*$^{-/-}$ MEFs at passage 2 and (C) in wild-type MEFs at the indicated passages. Percentages of input DNA are shown as the mean ± S.D. for three independent experiments.
doi:10.1371/journal.pone.0012373.g002

and H2AK119ub1, showed a significant reduction in the absence of Bmi1 (Figure 6B, D and G). Interestingly, the binding of Mel18 did not change, or actually enhanced, levels, suggesting a compensatory function (Figure 6C). Again, antioxidant treatment restored or enhanced the binding of Ezh2 and amount of H3K27me3 at the *Ink4a/Arf* locus (Figure 6F and G). In contrast, the binding of Ring1B was restored only partially (Figure 6B). These findings imply that Zfp277 functions as a platform for the Bmi1-containing PCR1 complex but not the Mel18-containing PRC1-like complex at the *Ink4a/Arf* locus.

Interaction of Zfp277 with Bmi1 is essential to maintain the life span of MEFs

To further confirm the requirement of physical interaction between Zfp277 and Bmi1 in culture-induced stress-resistance, we first determined the site where Zfp277 interacts with Bmi1 by co-immunoprecipitation using HA-tagged deletion mutants of Zfp277 and a Flag-tagged Bmi1 in 293T cells (Figure 7A). The N-terminal fragments (Zfp277$^{1-58}$, Zfp277$^{1-140}$) retained the capacity to bind to Bmi1, while the C-terminal fragment which lacked the N terminus (Zfp277$^{141-458}$) showed a significant reduction in capacity to bind Bmi1, indicating that the N-terminal portion, Zfp277$^{1-58}$, is the minimal region for interaction with Bmi1 *in vivo* (Figure 7B). We next introduced Zfp277 deletion mutants into *Zfp277*$^{-/-}$ MEFs and monitored cell proliferation. The expression of wild-type Zfp277 extended the replicative life span of *Zfp277*$^{-/-}$ MEFs, whereas the expression of Zfp277$^{141-458}$ did not (Figure 7C), despite that the mutant Zfp277 protein was expressed to the same levels of wild-type Zfp277 and retained a nuclear localization (data not shown). These findings underscored the crucial role of the interaction of Zfp277 with Bmi1 in the maintenance of the life span of MEFs.

Discussion

Our study demonstrated that Zfp277 is critical for the recruitment and/or stable accumulation of Bmi1-containing PRC1 at the *Ink4a/Arf* locus. The localization of Zfp277 was not dependent on the presence of specific PcG histone modifications, H3K27me3 and H2AK119ub1, or the PRC1 proteins Bmi1 and Ring1B. In contrast, neither the overexpression of Bmi1 nor expression of a Zfp277 deletion mutant which cannot bind to Bmi1 prevented the premature senescence of *Zfp277*$^{-/-}$ MEFs. These findings define Zfp277 as a platform for PRC1 and provide a novel mechanism for PRC1 to lodge at its target loci.

Studies in *Drosophila* have led to the identification of DNA regulatory elements that recruit PcG factors to chromatin, the so-called Polycomb response elements (PREs)(reviewed in Refs [11,21,40]). Pleiohomeotic-repressive complex (Pho-RC), which contains a zinc finger DNA-binding protein, Pleiohomeotic (Pho) or Pleiohomeotic-like (Phol), and Scm-like with four MBT domain-containing protein 1 (Sfmbt), directly binds to PREs and recruits PRC2 to PREs. While the study of mammalian PREs is in its infancy, two mammalian PREs, PRE-*kr* and D11.12 elements, have recently been identified, indicating conservation in the mechanisms that target PcG function in mammals and flies [41,42]. However, a global picture of PRE function in mammals has yet to emerge, and none of the recently characterized PREs have been shown to play roles in later cell survival or senescence. In mammals, PRC2 is recruited to PREs or target gene promoters by the sequence-specific DNA-binding protein yin and yang1 (YY1), the homologue of Pho in *Drosophila* [11,21,42]. However, it is unlikely that YY1 is generally required for the recruitment of PRC2 [42]. Instead, several transcription factors (TFs), such as Oct4 in ES cells, have been implicated as recruiters [11]. Furthermore, non-coding RNAs (ncRNAs) and Jarid2/Jumonji, a jumonji C family protein, have been proposed to interact with and recruit PRC2 to target genes [11,43]. Regarding the recruitment of PRC1, H3K27me3 induced by PRC2 serves as a binding site for CBX, one component of PRC1 [22]. Several CBX family proteins (CBX2, CBX4, CBX7, and CBX8) that have a highly conserved chromodomain can bind to H3K27me3 and participate in the PRC1-mediated transcriptional repression [44,45]. Nonetheless, it remains controversial whether CBX proteins target PRC1 directly to H3K27me3-marked chromatin [46,47]. Furthermore, accumulating evidence also suggests that PRC1 recruitment is not completely dependent on H3K27me3 [48]. In this regard, the precise mechanisms for the recruitment of PRC1 remain obscure. Based on our findings, we propose that Zfp277 participates in the recruitment of PRC1 to its target genes and the binding of CBX to H3K27me3 stabilizes the binding of PRC1 to chromatin. Whether this is generally true at all PcG target loci or only applicable to specific loci is an intriguing question to be answered.

Zfp277 contains five repeats of a C_2H_2-type zinc finger motif which is found in various transcription factors and capable of binding to specific DNA elements. Among zinc finger proteins, a POZ domain-containing DNA-binding protein, Plzf, is known to interact with Bmi1 and recruit it to target genes [49]. However, we do not know whether the zinc fingers of Zfp277 recognize any specific DNA sequences. It is well established that there is a cohort of zinc finger proteins with highly homologous structures. Therefore, Zfp277 could belong to a family of proteins with overlapping functions. Although the biological impact of *Zfp277*-deficiency awaits detailed analyses of *Zfp277*$^{-/-}$ mice, the fact that these mice are born healthy raises the possibility that the functions of Zfp277 can be compensated for by other family members *in vivo*.

Cellular senescence is a fail-safe mechanism protecting against genomic instability and tumorigenesis that can be provoked by intra- or extracellular stress. This cell-autonomous tumor barrier is often attributed to deregulation of the *Ink4a/Arf* locus. We have demonstrated that levels of Zfp277 protein are reduced in response to culture-induced oxidative stress through a proteasome-dependent pathway of degradation in wild-type MEFs. Furthermore, Zfp277 is immediately degraded when MEFs are exposed to UV and X-ray irradiation (data not shown), indicating that it is targeted by a broad range of stress-related pathways. Similarly, the accumulation of ROS triggers a reduction in PcG protein levels downstream of activated JNK signaling [50,51]. We also observed that levels of ROS in MEFs inversely correlated with levels of Zfp277 and PcG proteins. The fact that both Zfp277 and PcGs are crucial for repression of the *Ink4a/Arf* locus and inversely regulated downstream of stress pathways further supports that functional crosstalk occurs between Zfp277 and PcGs. Together, our findings indicate that PcG function is dynamically regulated in response to

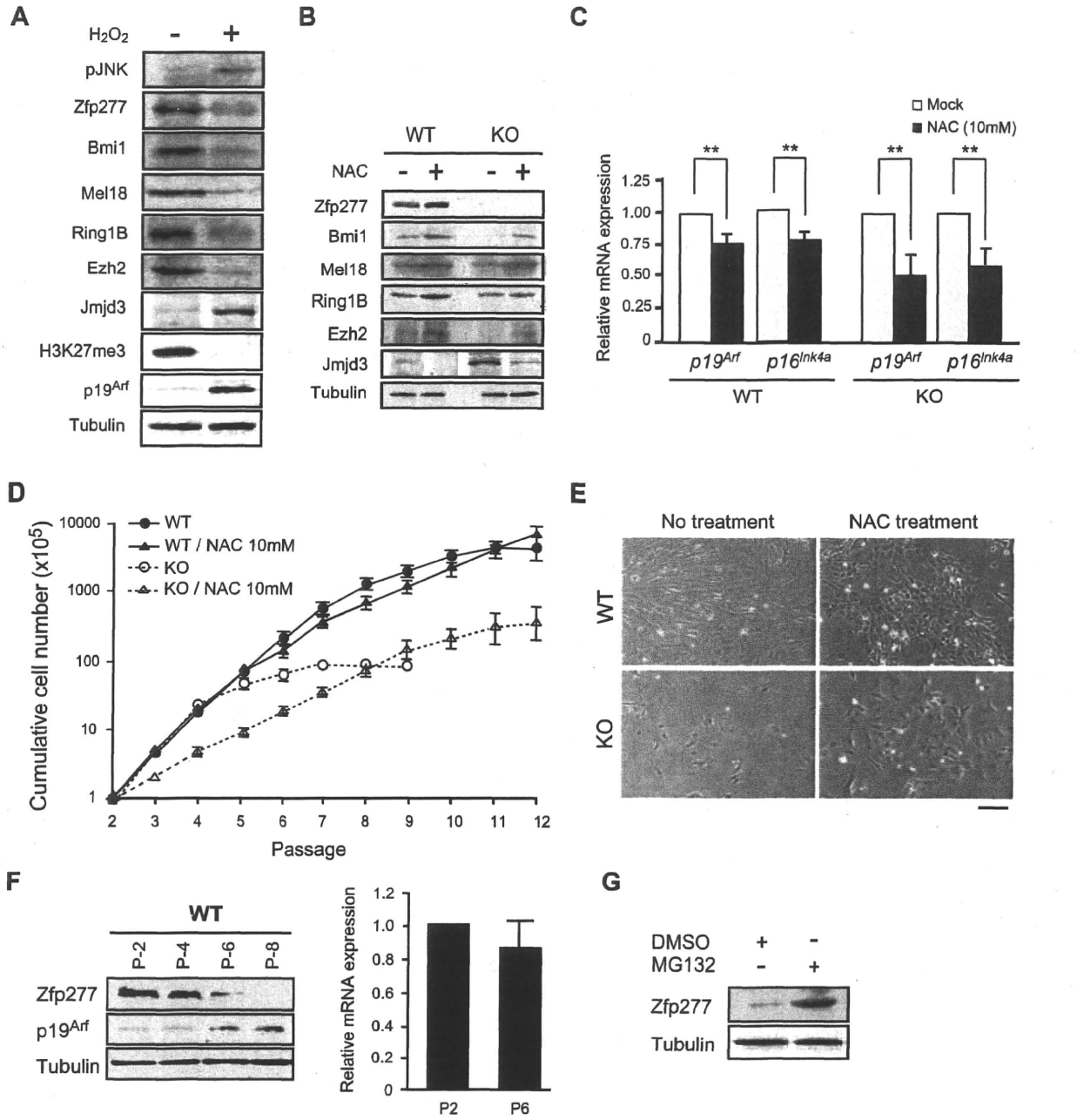

Figure 3. Oxidative stress leads to down-regulation of Zfp277. A. H_2O_2 treatment of MEFs. The whole-cell extract from wild-type MEFs treated with 100 mM H_2O_2 for 6 hrs was subjected to a Western blot analysis for the proteins indicated on the left. **B.** N-acetyl cysteine (NAC) treatment of MEFs. Wild-type and *Zfp277*$^{-/-}$ MEFs (P-2) were cultured in the presence of 10 mM NAC. MEFs were harvested at passage 6 and the levels of Zfp277 and PcG proteins were determined by Western blotting. Tubulin was used as a loading control. **C.** Quantitative RT-PCR analysis of *p19*^{Arf} and *p16*^{Ink4a} mRNA in wild-type and *Zfp277*$^{-/-}$ MEFs at passage 6 cultured in the presence of 10 mM NAC. mRNA levels were normalized to *Hprt1* expression. Expression levels relative to those in wild-type MEFs without NAC treatment are shown as the mean ± SD for three independent experiments. **D.** NAC treatment rescues the growth of *Zfp277*$^{-/-}$ MEFs. Wild-type and *Zfp277*$^{-/-}$ MEFs were cultured with or without 10 μM NAC and cell growth was monitored every three days by replating at 1×10^5 cells/plate. Cumulative cell numbers are shown as the mean ± SD for three independent triplicate experiments. **E.** Photomicrographs of wild-type or *Zfp277*$^{-/-}$ MEFs with or without NAC observed under an inverted microscope. Scale bar represents 200 μm. **F.** Expression of p19^{Arf} in *Zfp277*$^{-/-}$ MEFs. The protein levels of p19^{Arf} in wild-type MEFs at the indicated passages were determined by Western blot analyses (left panel). Tubulin was used as a loading control. Quantitative RT-PCR analysis of *p19*^{Arf} mRNA in wild-type MEFs at passages 2 and 6 (right panel). mRNA levels were normalized to *Hprt1* expression. Relative expression levels are shown as the mean ± SD for three independent experiments. **G.** MG132 treatment of MEFs. MEFs at passage 4 were treated with 10 μM MG132 for 6 hrs and Zfp277 protein levels were determined by Western blotting. Tubulin was used as a loading control. Statistical significance was determined with Student's t-test; $^{**}p<0.01$.

doi:10.1371/journal.pone.0012373.g003

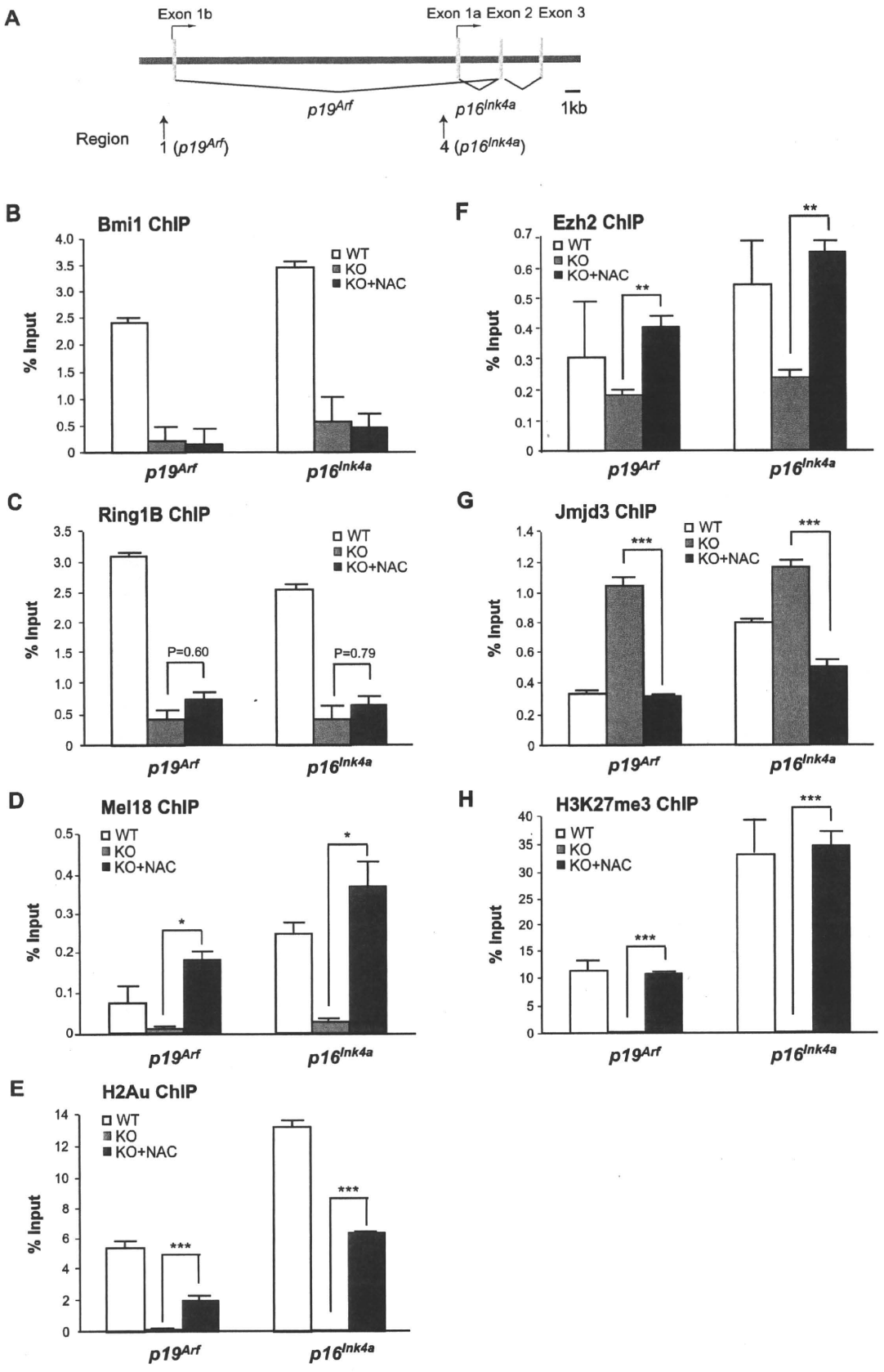
A
Exon 1b
Exon 1a Exon 2 Exon 3
p19Arf
p16Ink4a
1kb
Region
1 (p19Arf)
4 (p16Ink4a)
B
Bmi1 ChIP
WT
KO
KO+NAC
% Input
p19Arf
p16Ink4a
C
Ring1B ChIP
P=0.60
P=0.79
D
Mel18 ChIP
E
H2Au ChIP
F
Ezh2 ChIP
G
Jmjd3 ChIP
H
H3K27me3 ChIP